Aalto University
School of Chemical
Technology

School of Chemical Technology
Degree Programme of Materials Science and Engineering

Annina Eklund

CHARACTERIZATION OF STEP CUT CHIP DICING PROCESS IN MEMS ELEMENT MANUFACTURING

Master's thesis for the degree of Master of Science in Technology submitted for inspection, Espoo, 30 June, 2015.

Supervisor **Prof. Simo-Pekka Hannula**

Instructor **M.Sc. Eero Haimi**
M.Sc. Fang Tuurnala

Aalto University
School of Chemical
Technology

Aalto University, P.O. BOX 11000, 00076 AALTO
www.aalto.fi

Abstract of master's thesis

Author Annina Eklund

Title of thesis Characterization of step cut chip dicing process in MEMS element manufacturing

Department Materials Science and Engineering

Professorship Materials Science **Code of professorship** MT-45

Thesis supervisor Prof. Simo-Pekka Hannula

Thesis advisors / Thesis examiners M.Sc. Eero Haimi, M.Sc. Fang Tuurnala

Date 30.06.2015 **Number of pages** 85 **Language** English

Abstract

The goal of this research was to develop an optimized step cut chip dicing process for Murata Electronics Oy's acceleration sensing element wafer through process characterization. There was an interest to find out how different process variables affect the process output and how these variables can be adjusted to achieve the best possible dicing quality. The most critical quality issue had been the appearance of large back side chipping.

The characterization was carried out using a Design of Experiments (DOE) method to statistically analyse the effect of different variables. At first, a screening DOE was implemented to identify the most significant variables and then the process was fine-tuned with an optimization DOE. The input variables inspected in this research were blade type, step depth, feed rate and spindle speed. Outputs that were under interest were front side chipping, back side chipping, blade wear and spindle current. The chipping levels were evaluated with an optical microscope and an automated visual inspection device. Issues that were identified to lower the reliability of these results were the presence of uncontrollable factors, non-uniformity of the test material, lack of replicates and not inspecting the blade's behaviour throughout its lifetime.

Significant increase in dicing quality was achieved after process characterization and back side chipping levels were successfully reduced. The optimized step cut process was achieved with a metal bond blade, step depth 1/3, feed rate 7 mm/s, Z1 spindle speed 35 000 rpm and Z2 spindle speed 27 000 rpm. A shallower step depth, higher feed rate, lower spindle speed and a blade with softer bond material, larger grit size and lower concentration improved back side quality. Front side chipping in turn was reduced with a deeper step depth, lower feed rate and higher spindle speed. Blade wear and spindle current both increased by reducing spindle speed or increasing feed rate.

An undesirable outcome for the step cut process was a poor cut accuracy of the first cut blade. To further improve the process a blade with a smaller outer diameter is recommended to prevent the blade edge from bending and to improve the cut accuracy. Also the effect of a different mounting tape to achieve even better back side quality and die stability during dicing is under high interest.

Keywords MEMS, Silicon wafer, Dicing, Step Cut, Diamond saw blade, Chipping, Design of Experiments, Characterization

Aalto-yliopisto
Kemian tekniikan korkeakoulu

Aalto-yliopisto, PL 11000, 00076 AALTO
www.aalto.fi

Diplomityön tiivistelmä

Tekijä Annina Eklund

Työn nimi MEMS-elementtivalmistuksen step cut -sahausprosessin karakterisointi

Laitos Materiaalitekniikka

Professuuri Materiaalitiede **Professuurikoodi** MT-45

Työn valvoja Prof. Simo-Pekka Hannula

Työn ohjaajat/Työn tarkastajat DI Eero Haimi, DI Fang Tuurnala

Päivämäärä 30.06.2015 **Sivumäärä** 85 **Kieli** Englanti

Tiivistelmä

Tämän tutkimuksen tavoitteena oli kehittää optimaalinen step cut -sahausprosessi Murata Electronics Oy:n kiihtyvyysanturielementille karakterisoimalla sen prosessimuuttujia. Tarkoituksena oli selvittää miten eri muuttujat vaikuttavat prosessin ulostuloon ja miten näitä muuttujia voidaan säätää, jotta saavutettaisiin paras mahdollinen sahauslaatu. Merkittävimpänä laatuongelmana oli elementtien takapinnan murtumat.

Karakterisointi toteutettiin koesuunnittelumenetelmän avulla, mikä mahdollisti eri muuttujien vaikutuksen tilastollisen analysoinnin. Ensimmäisen koesuunnitelman avulla kartoitettiin olennaisimmat muuttujat, ja sen jälkeen tehtiin tarkentava koesuunnitelma, jossa selvitettiin lopulliset prosessiparametrit. Tarkasteltavat muuttujat olivat terätyyppi, stepin syvyys, sahausnopeus ja terän akselin pyörimisnopeus. Tarkasteltavat ulostulot olivat puolestaan etupinnan murtuma, takapinnan murtuma, terän kuluminen ja akselin virrankulutus. Murtumien kokoa mitattiin optisella mikroskoopilla ja automaattisella visuaalisella tarkastuksella. Tekijät, jotka laskivat tutkimustulosten luotettavuutta, olivat tuntemattomien muuttujien vaikutus, testimateriaalin epätasalaatuisuus, toistojen puute ja se että terän käyttäytymistä ei tutkittu koko sen elinkaaren ajan.

Sahauslaadussa saavutettiin merkittäviä parannuksia karakterisoinnin avulla ja takapinnan murtumaa saatiin vähennettyä. Optimaalinen step cut -sahausprosessi saavutettiin seuraavilla parametreilla: metalliterä, stepin syvyys 1/3, sahausnopeus 7 mm/s, Z1 akselin pyörimisnopeus 35 000 rpm ja Z2 akselin pyörimisnopeus 27 000 rpm. Pienempi stepin syvyys, suurempi sahausnopeus, pienempi pyörimisnopeus ja terä, jossa oli pehmeämpi sidosaine, isompi timanttikidekoko ja matalampi timanttikonsentraatio vähensivät takapinnan murtumaa. Etupinnan murtuma väheni suuremmalla stepin syvyydellä, pienemmällä sahausnopeudella ja suuremmalla pyörimisnopeudella. Terä kului enemmän ja akselin virrankulutus kasvoi, kun pyörimisnopeutta pienennettiin tai sahausnopeutta kasvatettiin.

Step cut -sahaus toi esille uuden haasteen. Ensimmäisen uran sahaava terä alkoi taipua sahauksen aikana, mikä ilmeni sahausuran siirtymisenä. Ongelman korjaamiseksi ehdotettiin ulkohalkaisijaltaan pienempää terää, sillä se voisi vähentää terän taipumista ja parantaa sahaustarkkuutta. Prosessia voitaisiin lisäksi kehittää esimerkiksi testaamalla erilaisten teippien vaikutusta takapinnan murtumaan ja elementin tukemiseen sahauksen aikana.

Avainsanat MEMS, piikiekko, sahausprosessi, step cut, timanttisahanterä, murtuminen, koesuunnittelu, karakterisointi

Foreword

This thesis was done at Murata Electronics Oy from January to June in 2015. I am grateful that I was given this chance to gain a deep insight into Murata's technology and to work closely with the industry experts. The more I learned the more interested I got. Now that this process has come to an end I realise how much work has been done and how many people have been involved. I want to thank you all for making this challenging yet pleasant project happen.

Fang Tuurnala for continuous support and for making it possible to stick to the schedule. Janne Kärhä for professional advice and help with carrying out the experiments efficiently. All the colleagues in the back end teams for giving me valuable hints and everyday support and for immediately considering me as a part of the team. Philip O'Leary for guidance with Minitab and for getting me interested in statistical analysis. Jussi Oksanen for brilliant SEM imaging.

I want to thank my supervisor Professor Simo-Pekka Hannula and my instructor Eero Haimi from our university for their support and for giving me essential advice from the academic point of view.

I would not be at this final point of my studies without my friends and family. You guys are priceless and you are the ones that always encouraged me to give my best and pushed me forward when most needed, not only during writing this thesis but especially throughout all the unforgettable years in the university.

Espoo, 29.6.2015

Annina Eklund

Table of contents

1 Introduction 1

1.1 The 3D MEMS technology of Murata Electronics 2

1.1.1 Product overview 2

1.1.2 Sensor measuring mechanism 4

1.1.3 Glass-silicon structure 6

1.2 Chip dicing of MEMS elements 8

1.2.1 Dicing process 8

1.2.2 Single, dual and step cut 11

1.2.3 Mounting 13

1.2.4 Blades 14

1.2.5 Dressing 18

1.2.6 Cutting parameters 20

1.3 Dicing quality defects 22

1.3.1 Chipping 22

1.3.2 Cutting accuracy 28

1.4 Dicing process characterization 30

1.5 The goal of the study 32

2 Research materials and methods 33

2.1 Materials 33

2.2 Experimental equipment 35

2.2.1 Fully automatic dicing saw 35

2.2.2 Optical microscope 36

2.2.3 Scanning electron microscope 37

2.2.4 Automated visual inspection device 38

2.3 Conducting the experiment 40

2.3.1 A Design of Experiments 40

2.3.2 Screening DOE 43

2.3.3 Optimization DOE 47

3 Results and Discussion 50

3.1 Screening DOE 50

3.1.1 Front side chipping 51

3.1.2 Back side chipping 55
3.1.3 Blade wear 58
3.1.4 Spindle current 60
3.1.5 Parameter choices after screening 64
3.2 Optimization DOE 65
3.2.1 Front side chipping 66
3.2.2 Back side chipping 67
3.2.3 Blade wear 70
3.2.4 Final parameter choices 71
3.3 Blade edge SEM inspection 72
3.4 Additional die geometry observations 77
4 Conclusions 80
References 82

Abbreviations

ASIC	Application Specific Integrated Circuit
AVI	Automated Visual Inspection
BSC	Back side chipping
DOE	Design of Experiments
ESD	Electrostatic discharge
FSC	Front side chipping
MEMS	Microelectromechanical system
SEM	Scanning Electron Microscope
UV	Ultraviolet

1 Introduction

Microelectromechanical system (MEMS) technologies have become an important area in the microelectronics industry. The demand and applications for MEMS devices expanded when mass production and miniaturization became possible in MEMS manufacturing. A MEMS sensor is a three dimensional silicon based structure which enables the conversion of physical quantities into electrical signals. The application variety extends from automotive and medical industry to consumer electronics like cameras and smartphones. [1] The wide range of MEMS devices includes accelerometers, gyroscopes, pressure sensors and optical devices [2].

This research was done at Murata Electronics Oy (MFI) which is company that designs and manufactures MEMS solutions for automotive, instrument and healthcare applications. This research was started in order to gain a deeper understanding of MFI's chip dicing processes and to find out what kind of quality improvements are possible through process characterization. The purpose of this research is to develop the dicing process of a 3-axis accelerometer sensing element. It includes the optimization of a step cut dicing process by performing a systematical process characterization procedure.

Chip dicing is a process step in MEMS manufacturing where the silicon based wafer is cut into individual chips. Dicing divides the front-end wafer level fabrication processes from the back end chip level processes. The most common dicing process for silicon based wafer manufacturing is mechanical diamond blade dicing. [3] The importance of good dicing quality has gotten attention for several reasons. In the manufacturing process the wafers have their highest value when they arrive to the die singulation step. Dicing does not directly add value to the product but it affects the packaging and assembly yield to a great extent. [4] A big challenge for MEMS dicing is that the structure includes insulating glass layers among the bulk silicon. Dicing glass and silicon in the same process is challenging due to their different response to mechanical cutting. This problem has been approached by a step cut dicing method which enables cutting different material layers separately. [5]

To perform a complete process characterization and optimization in dicing, a large number of variables need to be considered. Testing each variable separately is time and material consuming. An alternative method to the trial and error loop is a Design of Experiments (DOE). It reduces the number of trials needed to find out the combined effect of several parameters. [6]

The introduction part of this paper starts with introducing MFI's 3D MEMS technology and product variety. The next chapter explains the fundamentals of diamond blade dicing and introduces three different chip dicing methods: single cut, dual cut and step cut. Mounting, blade choice, dressing and cutting parameters are critical parts of the dicing process and their impact on the quality of a dicing process is discussed as well. The third chapter describes common dicing defects and the fourth chapter of the introduction part focuses on the characterization of a dicing process and the challenges that it faces.

1.1 The 3D MEMS technology of Murata Electronics

MFI manufactures, develops and markets accelerometers, inclinometers and gyro sensors mainly for automotive and healthcare industry but also for instruments and consumer electronics. MFI's 3D MEMS sensors are manufactured from monocrystalline silicon and glass and their operation is based on a capacitive measuring mechanism. [7] This chapter gives an overview of the structure and measuring mechanism of the devices manufactured with MFI's 3D MEMS technology.

1.1.1 Product overview

MFI utilizes multiple chip system-in-package encapsulation and connection technologies in their products. This means that a single sensor capsule contains one or more sensor elements and application specific integrated circuits (ASIC) depending on the product type. [7] The sensors are assembled by inserting the sensing elements and an ASIC into a pre-molded plastic casing, covering them with protective silicon gel and closing the case with a stainless steel lid. The appearances of the finished products are presented in Figure 1. The silicon gel protects the sensor elements from environmental impacts which make them highly insensitive to mechanical shocks and vibrations. Their reliability and performance remain stable even under changing temperatures and over long periods of time. [8]

Figure 1 An inclinometer (left), an accelerometer (middle) and a combined gyro sensor (right) manufactured by MFI. [8]

The 3D MEMS element that this research focuses on is a 3-axis accelerometer sensor that is used in combined gyro sensors. The exterior of a combined gyro sensor is showed in Figure 1. A combined gyro sensor includes both a gyroscope and an accelerometer and is used in demanding industrial applications in platform stabilization, motion analysis and navigation systems. [7] Especially in automotive markets there is a need to combine a gyro sensor with an acceleration sensor to be able to get a precise control of the vehicle posture. Legislations of installing multiple safety controls in new cars have become more and more common in developed countries. Electronic stability control, anti-lock brake system, tire-pressure monitoring system and hill start assist are essential functions where combined gyro sensors are needed. MFI already manufactures combined gyro sensor products and will continue enhancing its product lineup to meet the new demands. [1]

The structure of MFI's 3D MEMS devices basically consists of two capping wafers that seal the structural silicon wafer in between them. The moving parts such as the weights or comb electrodes are on the structural middle wafer and are attached to the frame portion by springs. [1] This structure can be seen in Figure 2 where an acceleration sensing element is separated into these three wafer levels.

Figure 2 An acceleration sensing element consist of top and bottom cap wafers and a structural wafer and has electrical contacts on the element surface. [9]

Two relevant features of the 3D MEMS devices are hermeticity and a via structure. The sensing elements are hermetically sealed on wafer level which means that the cavity in the MEMS structure is vacuum tight. No leakage is allowed over time. Hermeticity is a critical factor for devices that depend on resonance frequency stability. [10] The closed MEMS structure improves significantly the reliability of the sensor because particles or chemicals cannot access the structure after sealing. [7]

A via structure means that the electrodes are brought to the sensor element surface via a capping wafers. This makes it possible to extract the electrodes from desired locations which makes the design of the device even more flexible and simultaneously helps reducing the sensor size. [1] When electrical contacts of the sensor element are brought to the surface directly through the capping wafers it enables simple encapsulation and connecting techniques. [7] The electrical contact pads can be seen in Figure 2 on the die sidewall.

1.1.2 Sensor measuring mechanism

MFI's sensors are designed so that the total motion of an object is measured by the combination of six motions. Accelerometers sense the linear acceleration and gyroscopes sense the angular velocity. Parallel motion along X, Y, and Z axes are measured with accelerometers and rotational motion around each of the axes is measured with gyroscopes. [1]

A capacitive measuring mechanism utilizes capacitance to detect the movement of the sensor. Capacitance between two surfaces, the ability to store electrical charge, is dependent on their separation distance and surface area. Motions of the moving weights inside the sensor are detected by the change in capacitance in relation to the cap wafers or between the comb electrodes. When a movable part moves up and down it can be sensed with a cavity control technology of a high performance level. Between the movable part and the cap wafer there is a cavity of a few micrometers which enables the capacitance measurement. The cavity is created by a wafer that is exceptionally flat due to high precision polishing and wafer bonding fabrication technologies. [1]

The main operation principle of an acceleration sensor is that a weight supported by a spring moves in accordance with the acceleration speed and the motion is detected electrically by the change in capacitance. MFI's accelerometer has a unique structure that consists of four weights illustrated in Figure 3 which makes it possible to obtain information with one additional axis. It offers a higher degree of freedom with respect to the information measured from three axes: X, Y and Z. This technology makes the sensor extremely reliable for demanding automotive industry and other applications. [1]

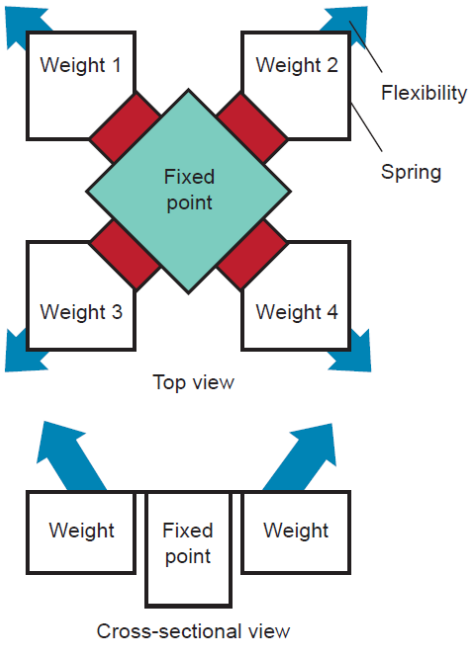

Figure 3 The operational structure of an acceleration sensor. [1]

The operation principle of gyroscopes is based on the detection of the force that on object experiences when it rotates around its own axis when it is moving in a straight line. This force, called the Coriolis force, is extremely small and that is why the most important thing in MEMS design is to cancel out disturbances coming from outside. In MFI's gyroscopes the pure Coriolis force is obtained with a unique structure of moving weights. Two weights are connected with a fine spring and they move in reverse phase (Figure 4). This movement is detected by obtaining information from four locations on the weights. By eliminating the linear and rotational acceleration in every direction with an arithmetic computation gives the pure Coriolis force as a result. [1]

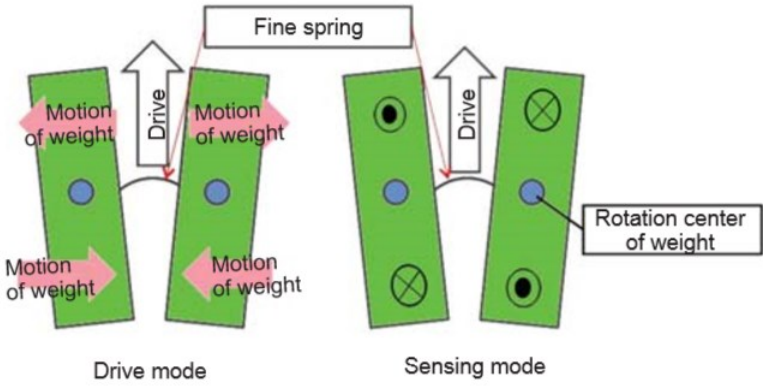

Figure 4 The operational structure of a gyroscope. [1]

1.1.3 Glass-silicon structure

Glass is used as insulation or packaging layers in between the silicon structure of MEMS devices [2]. The glass wafers used in 3D MEMS sensors are usually borosilicate glass. The reason for using this kind of glass is that its coefficient of thermal expansion is close to that of silicon. Thermal expansion is relevant because it is important for a successful anodic bonding process where the silicon and glass wafer are bonded together. The electrical behavior of glass in high temperatures is similar to semiconductors but the difference is that the charge carriers in glass are sodium ions not holes or electrons as in semiconductors. The sodium ionic conduction enables the anodic bonding process which happens in temperatures from 300 °C to 500 °C. For example in Pyrex glass the resistivity in room temperature is 10^{14} ohm-cm but in 350 °C the resistivity decreases to only 10^{6} ohm-cm. However, the properties of borosilicate glass vary a lot according to composition and the cooling rate during solidification. [10]

Glass is a metastable liquid and has no ordered structure in a larger range. The atomic structure of glass consists of a network of atom bonds between silicon and oxygen. Dopant atoms are located in the network either in substitutional or interstitial positions. Boron can form B_2O_3 oxide by substituting a silicon atom. Whereas, for example sodium, potassium and lead are located as interstitial atoms. They bond to a silicon atom with their only valence electron. Glasses do not have a specific melting point but they rather soften gradually. The melting properties are characterized by a transition temperature T_g where the behavior of glass changes from brittle-elastic solid to viscous melt. Transition temperature is defined as the temperature where viscosity equals $10^{12.3}$ Pa-s. Usually the processing temperature of glass is limited to 600 °C even though the softening happens at about 820 °C. That is because in wafer manufacturing even a slight change in the glass wafer shape may result in out of focus lithography or poor bonding. [10]

Combining glass with silicon in 3D MEMS manufacturing makes the dicing process more challenging. It complicates the optimization of blade selection and other process parameters. The glass-silicon ratio is dependent on the element design and the most relevant question concerning dicing is how the glass layers are located on the saw street. The number of glass layers and their thickness on the saw street highly affects the dicing process. The final process parameter selection is always a compromise between what would be the best option for dicing silicon and glass individually. There are different ways to approach these challenges and step cut dicing process is one of them. For example a step cut process where the glass wafer is first cut with a wider blade and the second cut through silicon is done by a narrower blade is proposed in a study by Ganesh [5]. Step cut method is introduced more closely in Chapter 1.2.2.

1.2 Chip dicing of MEMS elements

Diamond blade dicing is the most common dicing technique in the microelectronics industry. Chip dicing is a manufacturing process step where the sensor elements are singulated from the wafer by a mechanical process. The process flow from a bonded wafer to die bonding and wire bonding which are final assembly processes is shown in Figure 5. Dicing is a process that is affected by multiple variables such as mounting, blade type, blade dressing and several cutting parameters. These need to be adjusted separately for each dicing process to achieve the best possible quality. The fundamentals of a dicing process, different kind of cut methods and the most important process variables are represented in this chapter.

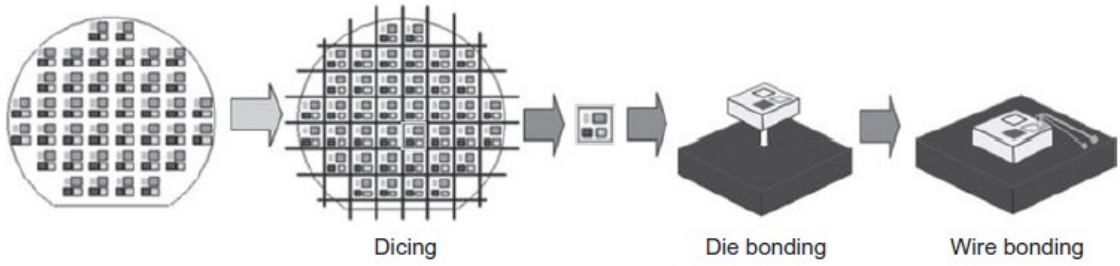

Figure 5 Process flow from a bonded wafer through dicing to the final assembly processes. [11]

1.2.1 Dicing process

Chip dicing is the process step that separates front-end wafer level fabrication processes from the back end chip level processes. This research is focused on mechanical blade dicing that is used for MFI's 3D MEMs manufacturing. The reason behind the popularity of diamond wheel dicing in the semiconductor industry is the good cut quality. It allows keeping multiple cutting parameters, such as cut width, cut depth, cut straightness and edge quality under precise control. [12] The wafers are prepared for blade dicing by mounting them on a tape frame which is then placed in a dicing saw. The wafer is moved under a rotating dicing blade which singulates the MEMS devices from the wafer (Figure 6). [11]

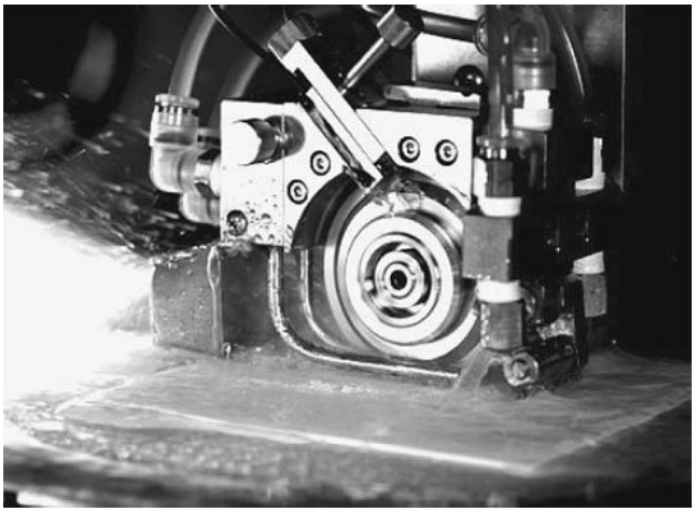

Figure 6 A wafer being diced mechanically with a diamond saw blade. [11]

Wafer dicing is performed with a dicing saw and there are various dicing saw models on the market to choose from. The machines can be operated either manually or fully automatically. The saw options include single-blade and multi-blade cutting, one and bi-directional cutting, different cooling nozzle alignments, spindle speeds ranging from 1 000 to 60 000 and different size blade mounting hubs. [3] A fully automatic dicing saw can complete the entire dicing process from loading to drying and unloading automatically. [13] The diced wafers are cleaned and dried in a high pressure washer before continuing to the next process step. [14] It is necessary to clean the wafers from dicing residue immediately after finishing the sawing process to prevent contamination like silicon dust getting stuck on the chips. The washer can either be a part of the saw or a standalone machine. [3] The silicon dust residue can stick to the terminal pads and reduce the strength and reliability of wire bonding. The dust may be hard to remove in the subsequent high-pressure cleaning operation but proper blade cooling and coolant nozzle alignment helps to prevent this problem. [6]

The cutting process in blade dicing is performed with a diamond blade attached to a high speed spindle. The cutting force of the dicing blade is based on abrasive synthetic diamond particles that apply stress levels on the substrate breaking the internal crystallographic bonds. The blade spins at velocities usually around 30 000 rpm which means the peripheral velocity of the blade is high. The blade is made of a matrix material that holds the diamond particles attached. Most common matrix materials are metal, nickel and resin bond and the matrix material should be chosen according to the dicing wafer material composition. The diamond

particle grit size and concentration are important factors affecting the cut quality. [15] More specific information about different blade options can be found in Chapter 1.2.4.

Flanges are the parts that mount the blade to the spindle. There are a back flange that is usually attached to the spindle and a front flange which is attached after blade change. The condition of the flange is important to check because a damaged flange will result in improper blade mounting. An incorrectly mounted blade can cause slanted cuts, blade vibrations, chipping or even blade breakage. For example a deformation on one flange side edge makes the blade bend to the other side. The inside diameter of back flange can also wear out over the time and cause loose fit on the spindle resulting in dynamic imbalance. If the flange is tightened too much or too loose the blade will wobble and not make an accurate cut. A major reason causing flange damage is particles flying around during the dicing process and therefore any defects should be checked from the flanges before dicing to ensure a good blade mounting. [16]

Dicing creates a significant amount of heat and therefore a proper cooling system is necessary to keep the abrasive diamonds at low temperature and thus the blade in good cutting condition. [17] Cooling of the blade and substrate material is an important part of the dicing process. Poor cooling can result in overheating and overloading problems. The cooling characteristics are influenced by the blade type, the quantity and alignment of the cooling nozzles and cooling pressure. [12] The cooling flow applies drag forces on the blade, which contributes to the blade torque. The latest dicing control systems are able to keep the torque effect of the coolant steady by controlling the coolant flow. [18] Increased cooling flow rate keeps the diamond particles on the blade edge residue free by washing away the cutting debris more efficiently. However, increasing the flow rate too high can result in liftoff of the dies. [19]

MEMS devices are extremely sensitive and fragile and effects such as contamination, vibration, heating, and electrostatic discharge (ESD) during dicing can cause device failure. [11] A processing error in dicing can turn a good quality wafer into thousands of pieces of expensive scrap. To begin with, a successful dicing process demands selecting the correct saw blade and achieving the best possible combination of control settings from dozens of options. Finding the correct parameters is dependent for example on wafer thickness, material composition, width of saw street, and die size. [3] In addition to difficulties in optimal process parameter selection blade dicing meets challenges such as vibrations caused by the high speed spindle,

contamination from the water coolant and silicon dust that may block the cavities and gaps. [10]

1.2.2 Single, dual and step cut

There are different dicing cut techniques to choose from depending on the capability of the dicing saw. The techniques are called single cut, dual cut and step cut and they are illustrated in Figure 7. Single cut is the most simple and common technique. Single cut is done with one blade and one spindle and the wafer is cut all the way through with a single pass. Dual cut and step cut both mean that the cut is performed with two passes. The first cut is done at a pre-determined cut depth and the following second cut goes through rest of the substrate. The difference between dual and step-cut is that dual cut refers to using one blade for both cuts so that the same blade passes through the same saw street twice. Step cut on the other hand is done by two different blades which are mounted in their own individual spindles, Z1 and Z2. [5]

Step cut requires a saw that has two spindles and is known as a dual spindle saw. In a dual spindle saw it is possible to give different spindle speeds for each of the spindles. One significant advantage of step cut dicing is the freedom to choose two different blades for the first and second cut according to the material layers diced on each cut. The first cut with Z1 can be performed with a wider blade so that the second cut with Z2 cuts only through the remaining substrate and into the tape. If the blade thicknesses differ there will remain a step in the die cross-section shown in Figure 7 c. Selection of the correct dicing technique depends on the wafer thickness and the saw street structure. Step cut is usually recommended for wafers with different layers of material on the saw street so that the sawing parameters can be optimized separately for each cut. [5]

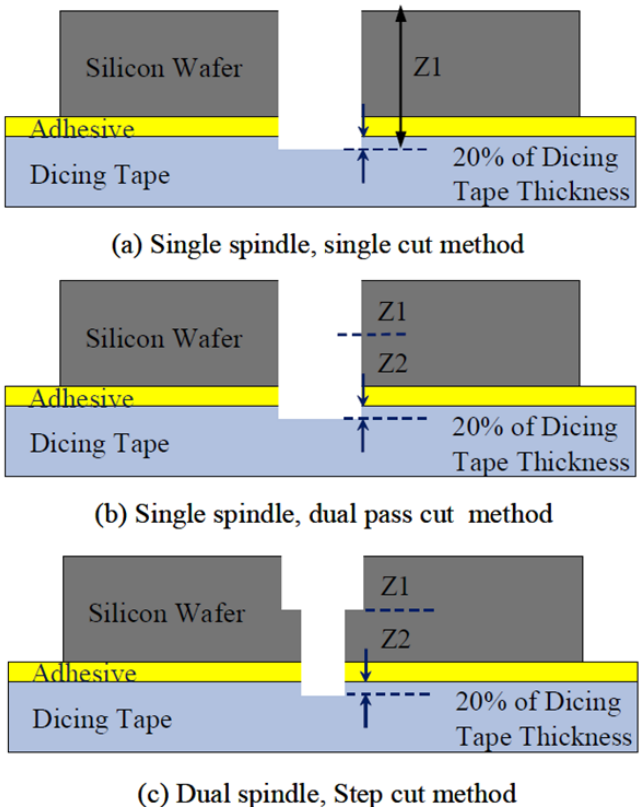

Figure 7 Single cut (a), dual pass cut (b) and step cut (c) are three different dicing techniques. [5]

Dual spindle saws were initially developed to increase throughput but they have been beneficial in reducing die front and back side chipping because of the freedom to choose different blades for each cut. The first blade is chosen according to the material layers in the kerf on the top side the wafer. The second blade is chosen for optimal cutting of the bulk semiconductor material. [20] In step cut dicing the first cut is a partial cut and its purpose is to reduce topside chipping to its minimum by refining the parameters for Z1 blade. The second cut is made into the remaining wafer usually with a thinner blade than the first cut and the cut goes through to a certain depth into the mounting tape. Back side chipping can be reduced by optimizing the Z2 second cut blade parameters. [4] In an article by Cheung [21] it was verified that step cut dicing reduced chipping and cracking in the die singulation process. Step cut process enhanced the cut quality because the first cut grooving relieved the stress in the wafer so that the second cut blade can saw the wafer with minimal cracking.

There is however some disadvantages for step cut dicing compared to single cut. Step cut requires a larger saw street width because the second cut demands certain placement

accuracy over the first cut which is usually wider. Step cut mode also reduces the process productivity by approximately 50 % if the feed rate is kept equal to single cut mode. [4]

1.2.3 Mounting

Wafers are mounted on a substrate during dicing to keep them firmly on place to be able to cut through as precisely as possible. A mounting tape is used for mounting the silicon wafer to a stiff circular frame. [3] The tape is fastened to a frame and the wafer is then placed on the adhesive mounting tape. The frame is a circular ring which makes the handling of the wafer easier. [16] The frame can be made for example of stainless steel or plastic [11]. A schematic picture of a mounted silicon wafer is shown in Figure 8. The contact between the tape and wafer should be as uniform as possible without air bubbles or any kind of particles between them. Poor contact can cause the dies to fall off during dicing. There are a large variety of tape thicknesses available with different adhesive thicknesses and strengths. [16]

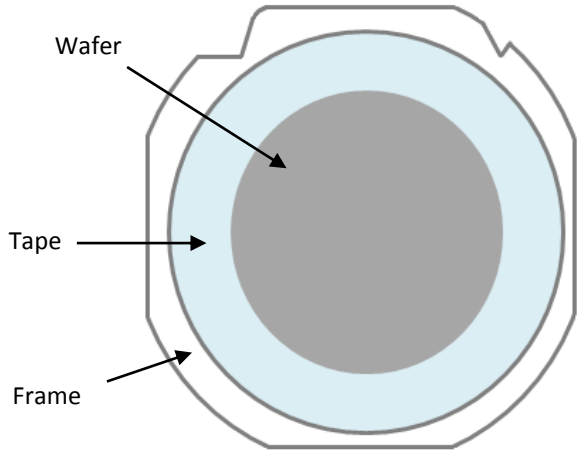

Figure 8 Wafer mounted on a dicing frame.

Most dicing tapes are made of polyvinyl chloride or polyolefin covered with an about 10 µm thick acrylic adhesive layer. [11] Two most popular tapes are blue film and ultraviolet (UV) tape. Blue film tape is more low-priced but has a limited adhesion value. UV tape has a much stronger adhesion before UV light exposure and a weak adhesion after the exposure. [3] An advantage of UV tape is that it makes the post-dicing die pick up easier. The dies can be easily

detached from the tape after been exposed to UV light because the light hardens the acrylic adhesive layer and makes the adhesion strength much lower. [11] UV release tape is often chosen because of its low tackiness and adhesion strength after exposure to UV light. [5]

The mounting tape has a large impact on die back side chipping because the tape material and the adhesive layer may clogg the blade edge and decrease its cutting efficiency. This effect is approached more closely in Chapter 1.3.1. Also poor mounting with air gaps or particles in between the wafer and the tape will cause chipping. [16] It has been shown that different mounting tapes affect wafer back side chipping according to the brand and peel strengths. [21] Wafer thickness and die size defines the dicing tape type to be chosen for the process. The smaller the die size the more challenging dicing becomes because then there is a relatively smaller area securely attached to the tape during dicing. In addition, in small dies chipping is more significant and obvious in relation to larger die sizes. [5]

1.2.4 Blades

Blade selection is a critical part in the dicing process. The blade type affects directly the cut quality and the choice of blade parameters have a big part defining the process time and costs. There are multiple blade parameters to choose from and each of them should be understood as closely as possible to be able to optimize the blades for different applications. [16] The cutting force of the blade comes from the diamond particles which are embedded in the binder material. There are many diamond particles on the blade edge and each of them cuts into the substrate material and removes it creating a kerf of a certain width and depth. [12] Two examples of a dicing blade are shown in Figure 9.

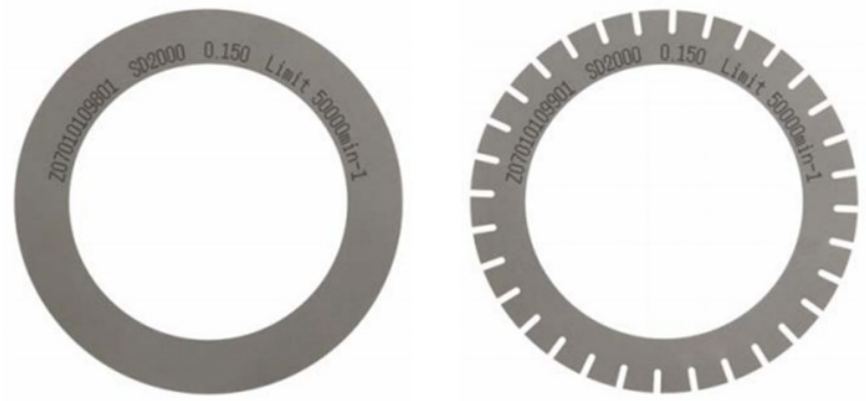

Figure 9 Different dicing blade types: a basic blade on the left and a serrated blade on the right. [22]

The binder material defines the overall softness or hardness of the blade. A metal bond, an electroplated bond or a resin bond matrix are examples of different binder materials. Production materials used in the microelectronics industry vary widely from soft to hard which means that a suitable blade needs to be chosen according to the process. Hard and brittle materials need to be cut with a softer blade which often means the selection of a resin bond blade. Resin bond blades stay in good cutting condition without a separate dressing process due to the soft binder that releases dulled diamonds and exposes new sharp diamond particles easily. [12] The downside of a resin bond blade is that it wears out fast but it is a good choice for achieving smooth chip free kerfs. The challenge for making blades for very hard and brittle materials in the microelectronics industry is the complexity of creating a soft enough matrix material that wears out fast to keep making clean cuts. It is dependent on the hardness of the phenolic resin matrix, diamond type and concentration, special fillers and other factors. [16]

Soft and less brittle materials need a harder blade such as nickel or metal bond blade. Nickel bond blade is even harder than metal bond blade and has a very low wear rate. Metal bond blade's hardness and wear characteristics are in between nickel bond and resin bond blades. A hard blade matrix results in longer blade life which means that the diamond particles need to be very hard to maintain their sharp edges through the whole life cycle of the blade. [12]

Bond hardness refers to the hardness of the binder that is used to secure the diamonds to the binder and it determines the loading level of the grits. The hardness defines the blade wear rate and self-sharpening mechanism of the blade. Soft bond wears fast but a too hard bond results in blade loading and cause chipping. [20] The overall hardness of the blade matrix consists of diamond grit size and diamond concentration in addition to bond hardness. Usually, finer grits, a higher concentration and a harder bond makes the blade matrix harder. When grit size increases, the impact of bond hardness to blade wear becomes less significant. However, the effect of diamond concentration to blade wear is relevant for all grit sizes. [18]

Using serrated blades are one option to reduce the load of the blade and enhance cooling. Serrated blades have slots all around the outer edge (Figure 9). Therefore, there is less contact between the blade and substrate which results in lower load and improved cooling in both the blade and substrate. The serrations also help to transfer the dicing residue away from the saw street. There are various serrated blades available with different serration sizes and quantities. One disadvantage of using serrated blades is the accuracy of the kerf width. Serrated blades

experience more vibrations than regular blades due to less contact area which can cause some inaccuracy in kerf width. [12]

Several characteristics of the diamond particle grits affect directly the cutting quality. Different grit sizes, concentrations and other grit features can be modified to reach the best quality for specific materials and processes. [12] The diamond grit size describes the size of the embedded diamond particles and typically ranges from 2 to 6 μm in blades for silicon wafer dicing. [3] The grit size defines the load and cut quality of the kerf. Larger particles dig deeper into the substrate and remove more material at once whereas smaller particles dig out less material and make a smoother cut surface. The material removal mechanism is illustrated in Figure 10. [23]

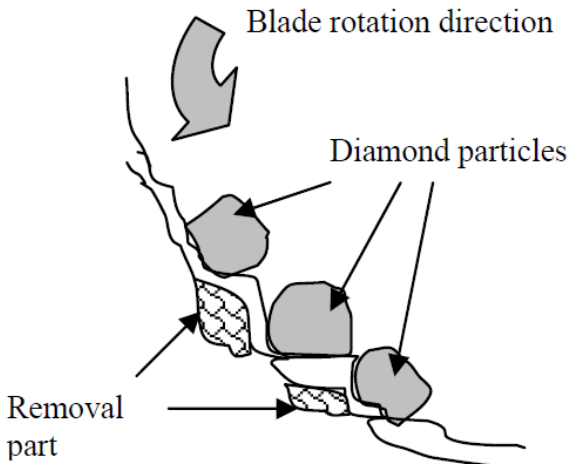

Figure 10 Material removal mechaniscm of the diamond particles on the blade edge. [23]

At a specific feed rate a smaller diamond grit size results in higher loads than larger grit size. Large diamond particles cause more chipping but are necessary for cutting hard materials to keep the loads on reasonable levels. Too small grit size can overload the blades, damage the material and even lead to blade failure or saw overload. [16] Diamond grit size regulates also the blade wear rate. Coarser diamond grits reduce blade wear significantly. [20]

SEM pictures of metal bond dicing blades with magnifications of 250x and 1000x are shown in Figures 11 and 12. The diamond grits can be seen as brighter areas on the blade surface.

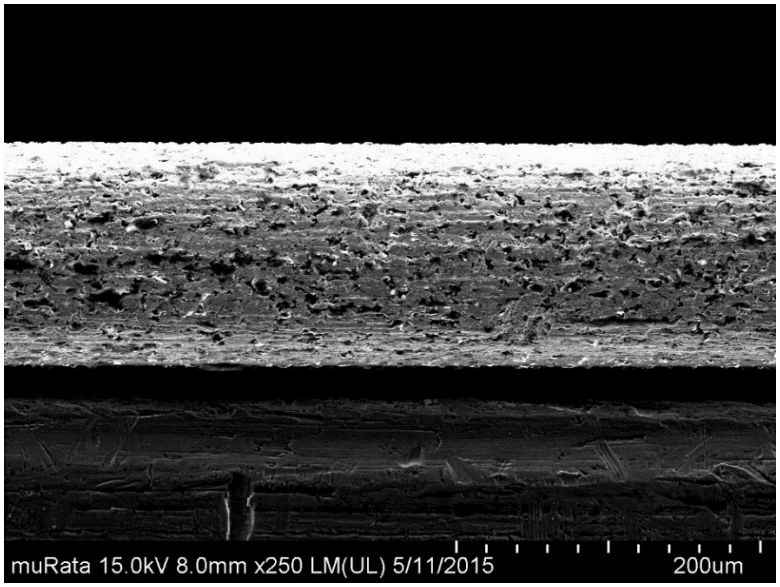

Figure 11 SEM picture of blade surface with 250x magnification.

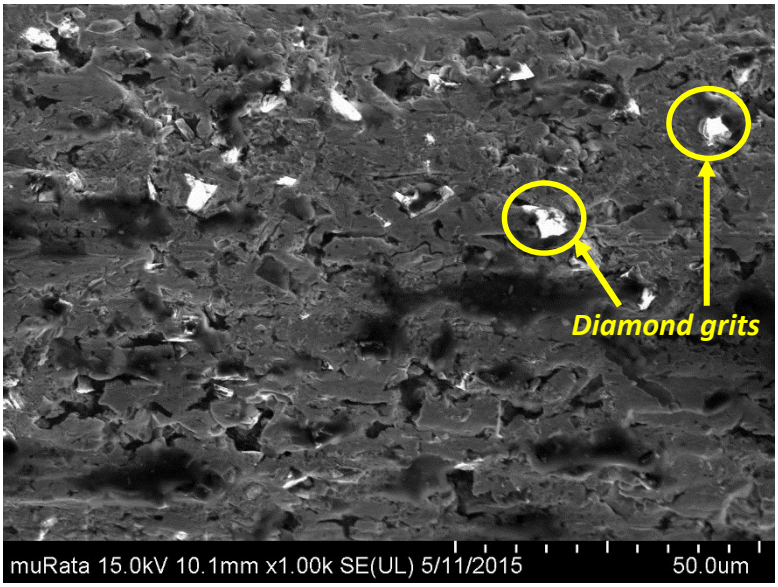

Figure 12 SEM picture of blade surface with 1000x magnification.

Diamond concentration is another factor that affects the cut quality and process time. A high diamond concentration makes the blade matrix harder and less wearing. A softer and more quickly wearing matrix is achieved with a lower diamond concentration. The cut quality is usually better with lower concentrations because the distance between diamond particles is then larger and there is more space to accommodate the dicing residue. Thus the cutting load is minimized. Diamond concentration also defines how well the blade edge keeps its original geometry. More particles at the blade edge results in a sharp edge with slower wear. [16]

Diamond particle shape and other features can also be regulated to optimize the blade characteristics. The most efficient diamond shape is a blocky sharp-edged particle because it is stronger than any other shape and it shows a more homogenous wear. It is possible to coat the diamond particles with another substance to improve the wear characteristics and help cooling the blade during the dicing process. [16]

1.2.5 Dressing

Suitable blade conditioning is another critical factor for achieving good dicing quality. Dressing is a conditioning process for saw blades which is made prior to dicing to produce a stable cutting force to the blade for dicing the actual production wafers. Dressing removes excess binder material from the blade surface and exposes new sharp diamond particles at the blade edge which makes the cutting more efficient. [24] An illustration of the blade edge before and after dressing is shown in Figure 13.

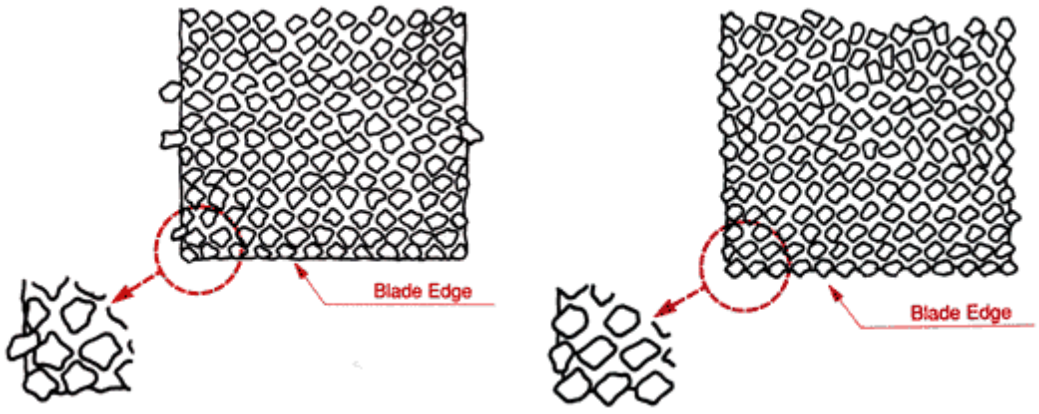

Figure 13 Blade edge before dressing (left) where the diamond grits are embedded in the matrix and after dressing (right) when new diamond grits are exposed. [12]

The abrasive diamond particles are embedded in the binder material after the blade manufacturing process. The purpose of dressing in addition to exposing sharp diamonds is to round the outside diameter, remove loose diamonds and flatten the blade edge. Every diamond particle acts like a single cutting tool in the dicing process and therefore they need to be exposed properly to be able to penetrate the substrate material efficiently and keep the cut quality at high level. Dressing helps to minimize the cutting load during sawing and to maintain a free and low temperature process. [25]

Usually dicing blades are edge-ground already in the factory but on-site dressing is still needed before using them in the dicing process. Dressing is performed on-site for all new blades and sometimes also during the dicing process. It depends on the specific dicing process and substrate material how often the dressing needs to be done. On-site dressing is essential because it improves the concentricity of the blade edge to spindle rotation, removes excess binder material exposing the diamond particles, warms up the blade and shapes the blade edge to suit the dicing process. The dressing board is located in the dicing saw either on an integrated dressing station or it needs to be placed in the machine manually before each dressing process. [25]

Dressing boards can be made of different materials and are available in different mesh sizes and geometries. [25] Silicon carbide dressing board was proven to be more effective than bare silicon wafer dressing. [26] The type of the dressing board needs to be selected according to the blade characteristics. Nickel and metal bond blades are hard and need proper dressing to stay in good condition whereas soft resin bond blades are self-sharpening because of the soft binder wears off easily. However, even resin bond blades require dressing in applications where the shape of the blade edge is critical. [25] Generally, a blade with finer grit size requires conditioning with a dressing board that has an equivalent or finer silicon carbide grit size. [24]

A well designed dressing process will pay off as good blade edge topography which impacts directly the blade profile, blade geometry, blade wear and cutting force. Parameters that need to be adjusted when designing a dressing process are material, feed rate, spindle speed, cut depth and the number of passes. [24] Dressing recipes made specifically for different blades has been proven to reduce the occurrence of chipping and other dicing related problems. [19] Novel blade load monitoring systems can provide force measurement to detect the desirable

end point of dressing. This helps to determine optimal dressing procedures and eliminates dicing with only partially dressed blades. [18]

1.2.6 Cutting parameters

Figure 14 shows the structure of a dicing spindle with blade mounting and some process related parameters. The load that is formed to the blade during dicing can be adjusted by changing the cutting parameters. [4]

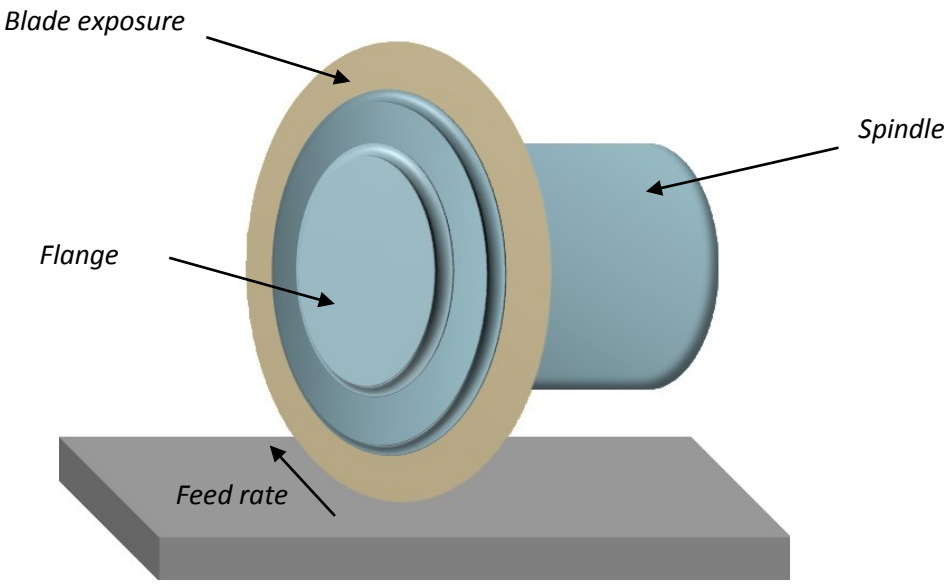

Figure 14 An illustration of dicing blade mounting and some related process parameters.

Feed rate is the speed that the chuck table moves under the blade and is measured in mm/s. Feed rate affects cut quality and should be optimized according to substrate material features and substrate thickness. A high feed rate means that larger quantities of material are cut off in a specific time and on each rotation. Blade load can rise relatively high if the feed rate is too high. Both the blade and the substrate can heat up to high temperatures in such circumstances. A high temperature further degrades the cut quality and shortens blade life. [16] Even though feed rate is kept constant during the process, variations in blade and wafer surfaces, such as diamond grit condition and saw street material, affect the cutting force during processing. [4] Usually a lower feed rate results in better cut quality. However, sometimes a too slow feed

rate makes poor cut quality because it generates more heat. For example back side chipping has been observed when dicing with very low feed rates. [18] Lei *et al.* [4] stated that cutting force increases as feed rate and dicing depth increase or when spindle speed decreases in the down-cutting mode.

Spindle is the part of the saw which rotates the dicing blade. Spindle speed is measured in rotations per minute (rpm). It is usually around 30000 rpm for silicon wafer dicing. A higher spindle speed means that each diamond particle will dig out a smaller portion of the substrate on each rotation and this induces bigger loads. A slower spindle speed in turn means that a single diamond particle digs out a bigger portion each time it touches the substrate. [16] Surface speed or cut speed, v is the linear rate of travel of the blade and it takes into account the blade diameter and spindle speed according to Equation (1). Die edge chipping levels can be regulated by adjusting the surface speed. Higher surface speed decreases blade life and makes cooling of the blade more difficult. [20]

$$v = \pi \cdot D \cdot N \tag{1}$$

where *D = blade outer diameter*
N = spindle speed

Cut depth is a process parameter that becomes more relevant in dual cut and step cut processes. In single cut the only cut depth that needs to be determined is the depth into the mounting tape. Step cut is usually performed with a dual spindle saw where two different blades are passing the same saw street and both of their cut depths need to be determined. The first cut depth is usually set to 50% of the wafer thickness but it can be optimized anywhere from 25% up to 75%. The 50% is chosen often so that systemic tolerances such as height variations can be taken into account. The second cut goes through the remaining wafer and a typical cut depth is around 20-40 μm into the mounting tape. [19] The cut depth into tape is preferably around 25 to 40 % of the tape thickness. This depth is large enough to avoid the lip effect on the die back side but small enough not to weaken the tape causing tearing in

later process steps such as die pick up. [21] Cut depth affects also blade loading because cutting through a thicker substrate results in higher loads. [16]

Blade exposure is the height of the exposed part of the blade that is available for cutting into the workpiece. It is dependent on blade outer diameter and flange diameter. Blade exposure needs to be large enough to be able to cut through the wafer and into the mounting tape to a specific depth. [3]

1.3 Dicing quality defects

Yield loss due to damage caused by the dicing process is an issue that needs further improvements in the semiconductor industry. [27] Dicing defects have been proven to lower the results of post-dicing reliability tests and defects that form during dicing appear later on and cause problems such as die cracking and wire bonding issues. The quality of a dicing process is mostly measured by the yield loss it causes in following process steps. [5] Most common dicing defects are chipping of the die edges, cut surface damage such as roughness or scratches and undesirable die geometries. [15] When the defects reach the active areas of the dies it results in malfunction of the device. Several dicing parameters need to be optimized to relieve the wafer stresses that are causing these defects. [27] The most relevant quality defects in this research, chipping and cutting accuracy, are introduced more closely in the following chapters. Chipping is further divided into front side and back side chipping.

1.3.1 Chipping

Die edge damage in which small pieces of material comes loose from the surface is referred as chipping. Microcracks are initiated under stress induced by the sawing blade and chipping happens when microcracks propagate and join together. [17] Chipping may occur both in the front side and back side of the wafer. Silicon and glass are very different kind of materials but they both behave as brittle materials during cutting. That is why dicing these materials result in microcracks in the die sidewalls and as chipping at the die edges. Minimizing these defects has been a priority target in back end fabrication processes. [17]

Chipping acts as a stress concentration site and therefore is a cause of die cracking and fracture in later process steps. This affects yield and is therefore an important quality factor

that should be controlled and improved. [4] Edge chipping creates stress-risers which cause die cracking and it finally results in reliability problems of the device. Also chip bending due to mismatches in material expansibility during temperature variations can lead to brittle fracture propagation originating from the die edge cracks. [20] Even though there are multiple variables affecting chipping in the die singulation process a few main variables can be defined: internal stress of wafer, blade selection, mounting tape and feed rate. [21]

Silicon is a brittle material which means that its fracture strength is lower than its yield strength. Under tensile load or bending silicon fractures before any plastic deformation happens due to relatively immobile dislocations at room temperature. Machinability and workability of brittle materials are affected especially by low fracture toughness and hardness. Silicon is crystalline material that crystallizes in the cubic diamond lattice. [28] Silicon's behavior under high loads during dicing is explained by the mechanical response of silicon. Each time the mechanical machining tool passes the wafer it leaves a damaged region below the machined surface. Plastic behavior is considered when the following cut removes material only from the damaged region resulting in relatively chip free and smooth cut surface. Brittle behavior occurs when more material than the damaged region is removed or a large local damage area has been induced. Brittle behavior can be recognized from crack initiation and chipping. [15]

For a brittle solid material there is a material specific factor that predicts the stress intensity near the tip of a crack caused by a load. The factor is called critical stress intensity or fracture toughness, K, and is defined in Equation (2). The value depends on material crystal orientation, doping concentration and temperature of the material. For silicon the critical stress intensity is approximately 1.1 MPa$\sqrt{\mathrm{m}}$. For a given load it is the defect size that defines the critical K. A crack will propagate when the critical value is exceeded. The total applied load is a sum of different stresses applied by the cutting process itself, residual stresses introduced during dicing and residual stresses left in the wafer by earlier fabrication processes. The stresses related to the cutting process can be regulated by changing feed rate and spindle speed. The residual stresses that origin from earlier process steps can be very high and their presence explain the quality differences between wafers even though they are diced with the same machine and same parameters. [15]

$$K = \sigma\sqrt{\pi r} \quad (2)$$

where σ *= the applied stress (Pa)*

r = the size of a defect (m)

The crack propagation direction depends on the applied load, residual stresses and the orientation of the defect. On the grounds of these matters, chipping damage can be prevented by keeping the defect size within the depth of the plastic zone and the local loads low enough so that the critical stress intensity is not exceeded. [15]

Monocrystalline semiconductors are typically fragile and express brittle behavior in mechanical machining. They exhibit limited dislocation mobility below 650 C. However, new research on the subject has shown that under particular conditions of depth of cut it is possible to achieve ductile material removal mechanism and crack free surface. This happens by shear involving mechanisms of slip system activation and dislocation movement. Experiments have demonstrated that diamond cubic structure of silicon transforms to metallic structure under pressure and reverses into an amorphous phase with a cubic structure when the pressure is released. [29]

1.3.1.1 Front side chipping

Front side and back side of the wafer act differently during dicing and damages are caused by different reasons depending on the wafer side. Front side is the wafer surface which the rotating saw blade hits first and backside refers to the surface that is attached to the mounting tape during dicing. Front side chipping (FSC) is mainly caused by the impact of diamond grits hitting the top surface. The impact of a single diamond in a rotating dicing is illustrated in Figure 15. FSC commonly consists of relatively small equal size cracks along the die edge. Also larger shell shaped chipping is possible because brittle materials often break off leaving a dimple that is shaped like a shell. [16]

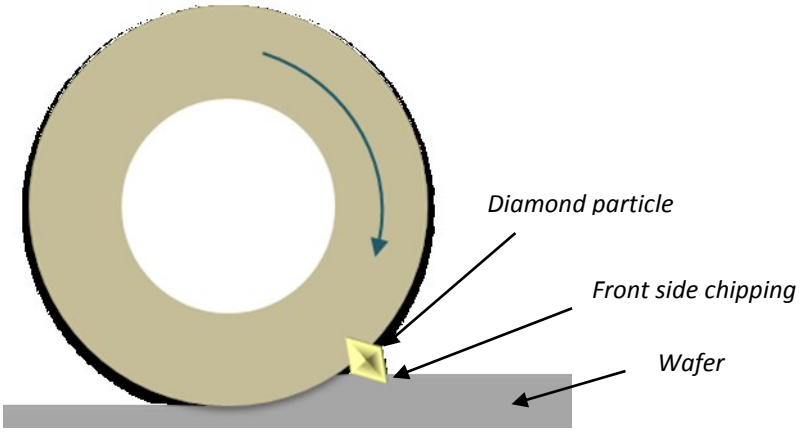

Figure 15 Front side chipping forms when diamond particles hit the top side of the wafer.

A research showed that to obtain good front side quality the wafer should be processed at a lower spindle speed and with a deeper cut into the silicon wafer [26] Feed rate affects straightforwardly the chipping size because higher feed rates cause higher temperatures and higher loads due to diamond grits removing larger amounts of material on each rotation. A softer machining mechanism is profitable for front side quality. Diamond grit size has a significant impact on FSC. A larger diamond grit size has been proved to increase FSC because it causes a higher impact force on the wafer surface. Coolant flow is also a notable reason behind FSC. [20] Additional factors that are recognized to affect FSC are blade vibrations and poor mounting. [16]

Lin and and Cheng proved in their research that changes in blade surface condition during dicing highly affects FSC. When blade surface roughness increased the chipping size increased as well. Diamond grits detach from the blade leaving holes on the surface which increases the surface roughness momentarily. The heights of the grits become more even when the process moves on decreasing the surface roughness. Therefore, the blade produces different cut qualities according to the blades surface roughness. [30] One suggestion to control this kind of variability is to replace the blade more often so that it is constantly in good condition but this adds costs and decreases productivity [4].

1.3.1.2 Back side chipping

Back side chipping (BSC) is formed when irregular micro-cracks propagate away from the bottom side and join together. Long enough microcracks cause pieces of silicon to detach from the die edge. BSC reduces yield if the micro-cracks reach a certain length that makes the dies sensitive to thermal cycling and lowers their reliability. BSC appears more if there is metal layers on the dicing streets or if the wafer back grinding process has produced high tensile residual stress at the bottom of the wafer. [18] BSC is caused partly by the same reasons mentioned for FSC but mainly due to a few other reasons. Stresses that are formed on the wafer back side in previous process steps are released during dicing and they are the cause of back side chipping. [18] The wafer structure is usually fixed so the tools for a process engineer for back side chipping control are limited to blade selection and process parameters optimization. [6]

During cutting the blade produces a propulsive force that pushes the two wafer sides apart. This movement causes forces to the back side of the wafer which is attached to the tape. Therefore, the die edges crack when dicing through the wafer. The separated dies are no longer supported as firmly as on the undiced side of the wafer. The separated side moves more than the rest of the wafer due to the forces that it experiences which causes more back side chipping and poorer cut surface quality. This kind of formation of back side chipping is illustrated in Figure 16. Additionally, process conditions such as poor cooling, a too slowly wearing blade or a defective blade causes exceptional back side chipping. [31]

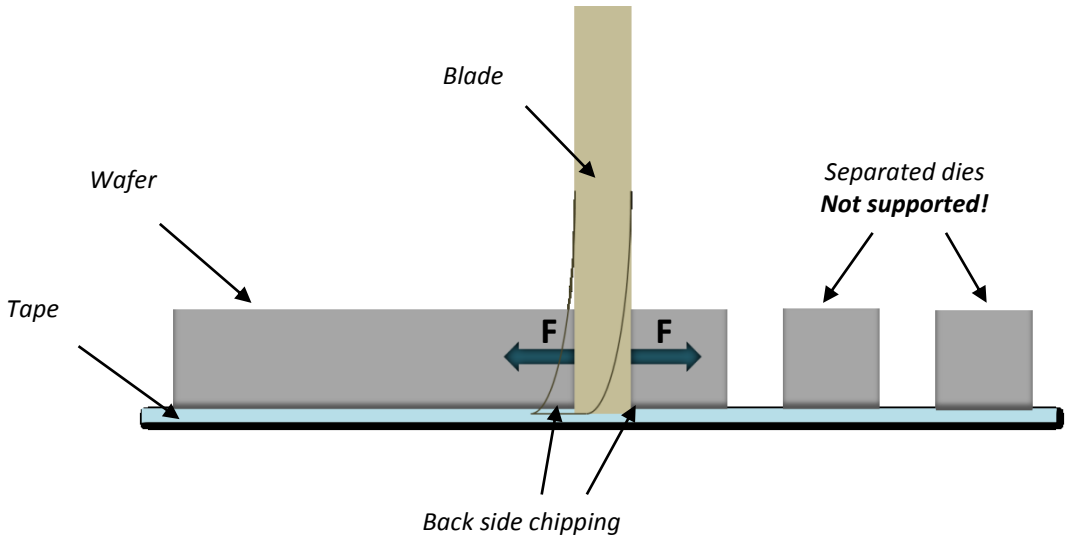

Figure 16 Forces causing back side chipping.

The mounting tape is a big factor affecting back side chipping because it can clog the blade edge raising the temperature and overload the blade. If there is some air gaps between the tape and the wafer the back side is not supported properly and it will cause chipping. [16] Polymeric material from the mounting tape clogs the blade edge by sticking to the free space between the diamond particles. A clogged blade has negative consequences as it makes the blade edge dull and blocks the free paths for cutting debris to move. The loosened diamond grits do not come off easily from a clogged blade and the cutting debris is pushed against the kerf sidewalls. These problems overload the blade and cause severe chipping, slanted cuts, blade vibrations and microcracking. [4] There are a few ways of minimizing the possibility of blade overloading in the tape. Larger diamond grit size and an appropriate cooling system can be helpful. Slowing down the feed rate is also one option. [16]

Another reason behind back side chipping is the lip effect. If the cut into tape is not deep enough or the blade edge radius has become too large it leaves a lip on the back side die edge. This lip can either stay on the die causing incorrect geometry or crack of the die causing large size BSC. The lip effect is demonstrated in Figure 17. To eliminate this issue the blade edge should be maintained flat with a small enough radius on the edge. An optimal blade matrix, cutting parameters and blade dressing during dicing is important in achieving proper blade condition throughout the dicing process. A thicker tape can also reduce the lip effect because then it is possible to cut deeper into the tape. [16]

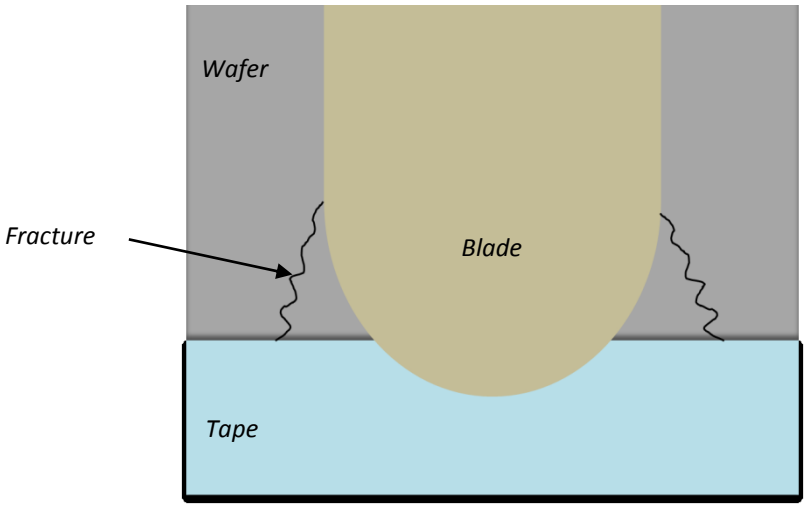

Figure 17 The lip effect happens due to a large blade edge radius.

A couple of methods are known to reduce BSC such as a reduced feed speed and using a step cut method. Blade selection is important and with step cut dicing the blade for surface and bulk material cutting can be selected serparately. Some other factors that are known to affect BSC are blade height, blade cooling, unstable support, spindle vibration or any combination of these factors. [20] Softer blade bond material and a lower diamond concentration are also suggested to improve BSC levels. [18] The appearance of BSC is found to correlate with blade torque which is affected by the combination of all process variables. Above a certain torque limit the dicing quality decreases and more BSC appears. If a real time torque measurement is possible in the dicing saw the torque limits can be adjusted and controlled for each process which would help to eliminate excessive blade loading. [6]

1.3.2 Cutting accuracy

Kerf width, index step and depth of cut of a wafer are illustrated in Figure 18 to give an idea how the adjustment of these parameters affect the final outcome of the individual dies. These parameters are inserted to the dicing saw recipe and can be specified for each product separately. Also kerf geometry and cut placement accuracy during dicing affect the final size and shape of the dies.

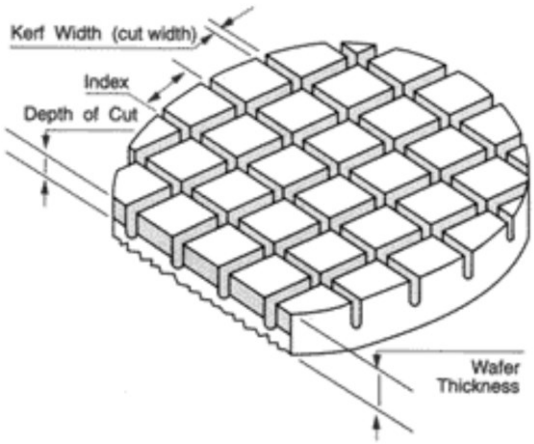

Figure 18 Parameters defining the die geometry. [12]

Kerf geometry consists of kerf perpendicularity and kerf width. Kerf perpendicularity includes measures such as the tilt of the cut, kerf taper and back side lip effect. The appearance of these defects is especially critical for product types where the sidewall of the die is functional in the end product. [4] A few common examples of undesired kerf geometries, a slanted cut, a tapering cut and an asymmetric chamfer, are presented in Figure 19.

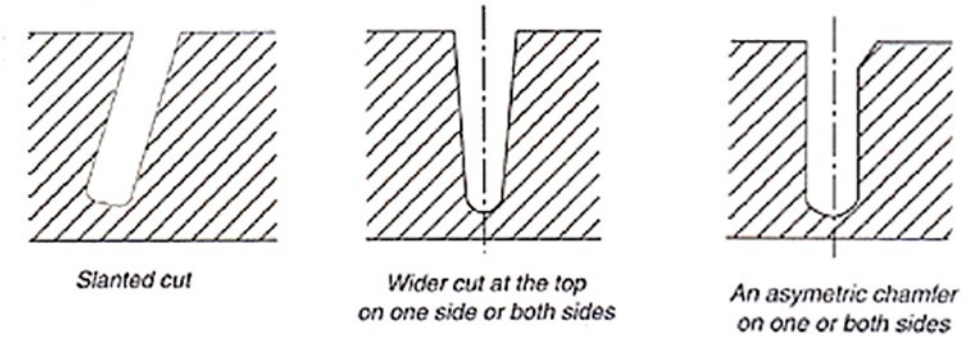

Figure 19 Undesired dicing kerf geometries [16].

The correct blade thickness is determined by the width of the saw street and desired kerf width. [3] Kerf width control is important when trying to achieve the minimum saw street width and low variation. This would make it possible to increase the number of dies on a wafer and make the process more effective. [4] Kerf width can turn out to be wider than the blade width if the blade is not accurately aligned with the feed motion or due to axial vibrations. Blade defects such as protrusions can also cause wider kerf widths. Vibrations are due to minor imbalances in the blade assembly and they make the blade vibrate in its plane when it rotates at high velocities during cutting. Efrat's experiment showed that radial vibrations had no effect on chipping under the tested conditions but they might have an impact on kerf width, blade life and other variables. The observation was explained by an insignificantly small radial displacement of the blade. [15]

Cut placement accuracy is a function between the saw vision and positioning systems. If the cut placement has not been correctly adjusted in relation to the saw street or it has moved during dicing it can result in damage to the active die area or in undesirable die shape. [15] Cut placement accuracy, also known as cutting offset or kerf straightness, measures the waviness of the kerf. In other words, it measures the difference between center of the kerf and center of the sawing street. [4]

1.4 Dicing process characterization

The target in silicon wafer manufacturing is to increase throughput and yield while minimizing cost of ownership. Optimization of the dicing process aims at achieving the best possible quality with the highest possible throughput. The dicing throughput is measured by the number of wafers diced in a specific period of time. To reach a high throughput in dicing it requires using as high a feed rate as possible. The challenge is that usually when the feed rate is increased it becomes more difficult to obtain a good dicing quality. [18] One relevant factor affecting the process output is also that the cutting quality starts to vary when the blade wears during the dicing process. Therefore, cutting quality should be kept under control through the whole life cycle of the blade. [4]

There are a remarkably high number of variables affecting the dicing process and it would not be reasonable to try and study all of their effects at once. All the parameters should be adjusted together to achieve the most optimal dicing result. The fishbone diagram in Figure 20 reveals the extent of parameters affecting the dicing process. The parameters that usually get the most attention are feed rate, spindle speed, cooling flow rate, cooling alignment and depth of cut. [14]

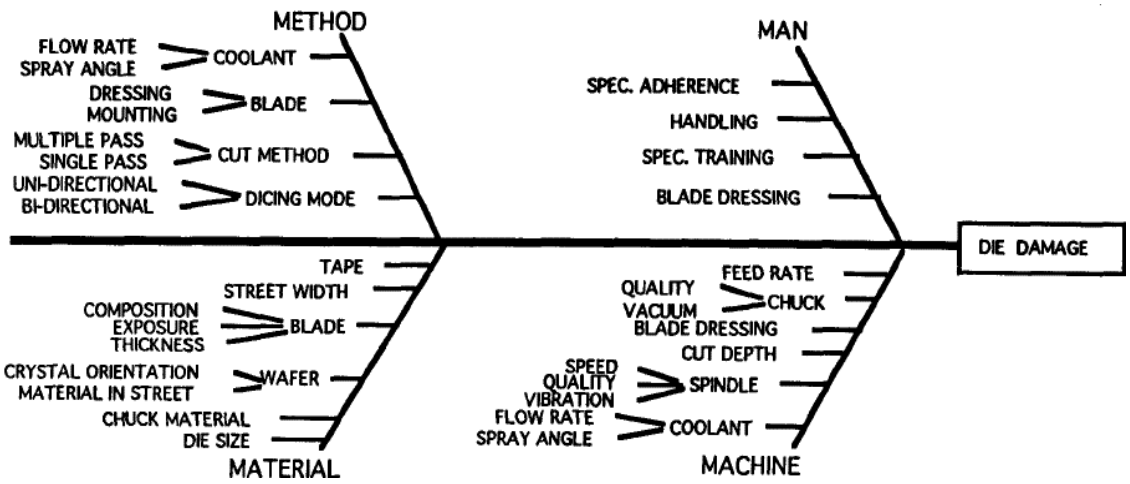

Figure 20 A fishbone diagram illustrating the extent of parameters affecting a dicing process and causing die damage. [14]

In a research by Efrat it was found out that blade vibrations, cooling alignment and dressing method did not have a significant impact on chipping under the tested conditions. Instead, the effect of cooling flow rate, spindle speed and feed rate were found more notable. Chipping

was more affected by the substrate material and blade type than any process parameters. [15] Finding the optimal dicing parameters usually starts with finding a suitable blade type and then continues with tuning the cutting parameters. [31]

The purpose of optimizing the dicing parameters is to decrease dicing defects which means finding the optimal cutting force required to break the internal crystallographic bonds of the substrate material. [15] Too high or insufficient cutting force will result in an unsuccessful dicing outcome for example as chipping or blade breakage. The dicing process parameters need to be chosen according to how much material need to be removed by the blade and are highly dependent on blade properties. [5]

To achieve better yield and productivity it is necessary to increase accuracy of dicing and to create new control capabilities. The main limitations in increasing feed rate are larger chipping rates and yielding of the blade. To be able to determine the maximum feed rate without exceeding blade limitations, a special control method for blade torque measurement has been recommended. [6]

Wafer dicing is a process affected by dozens of variables and it is therefore highly challenging to do Design of Experiments of all the variables and get reliable and unambiguous results. Even so, for example careful selection of dicing saw parameters, blade type and mounting tape has been proved to result in substantially reduced chipping. [21] Process characterization includes usually sequential Designs of Experiments but even after careful experimentation the conventional characterization process does not take into account the machine-to-machine variation and the time instability of machines. The downside of a typical process characterization is that the trial runs are usually conducted with a single machine and using one single batch material. Any variation in processing material or machine will drift the optimized process window. This may give rise to problems when shifting into production runs due to a different machine and a higher quantity of material being processed compared to engineering run. These issues will affect the stability and predictability of the process but are extremely hard to find out during engineering runs. [32]

1.5 The goal of the study

This research was started because of the need for a deeper understanding of MFI's chip dicing processes. It was under interest to seek possible dicing quality improvements through careful and systematical process characterization. With MFI's MEMS products the challenge in dicing is not only to understand how silicon acts during dicing but also to understand in which ways the glass layers in between affect dicing. New products are continuously developed and the requirements for dicing accuracy increase along them. The uniqueness of every dicing process and every product makes it extremely challenging to apply information gained from previous studies to these new processes.

This study focuses on optimizing the chip dicing process of a 3-axis accelerometer sensing element used in combined gyro sensors for industrial applications. The most critical dicing quality issue for this product is the appearance of large back side chipping partly due to the glass layers on the dicing streets. A new step cut dicing method has been introduced to reduce the amount of back side chipping. The aim is to be able to replace the old single cut production process with an optimized step cut process after performing this research.

The goal of this research is to characterize the step cut dicing process and to find the optimal parameter combination to achieve the best possible dicing process for the acceleration sensing element. The questions to be answered are in which ways different process variables affect the process output and which process parameters should be chosen to reach the most optimal dicing quality. The process characterization is carried out by Design of Experiments (DOE). The process variables considered in this study are blade type, feed rate, spindle speed and step depth and the inspected process outputs are front side chipping, back side chipping, spindle current and blade wear.

2 Research materials and methods

This chapter includes information about the materials and methods that were used in this research. Materials are listed in the first chapter and after that the experimental equipment is introduced. The final chapter of this section introduces the Design of Experiments method and describes how the experiments were carried out.

2.1 Materials

The materials needed for the experiments are listed in Table 1.

Table 1 The materials used in the experiments of this research.

Material	Information
Processed silicon wafers	- thickness: 825 μm - include glass layers
Dicing blades	- two different metal bond blades - nickel bond blade
Dressing boards	
Dicing tape	- UV curable - strong adhesion - thickness: 150 μm
Mounting frame	

Processed silicon wafers of 825 μm thickness were used as test material in this study. The wafers had been processed similarly to normal production wafers until they reached the dicing process step. Some minor differences in the previous process steps are possible compared to normal production but the wafer structure on the dicing streets was the same. Total of 24 silicon wafers were diced in this experiment. 16 silicon wafers were used for the screening DOE ad 8 wafers were used for the optimization DOE. The wafers included glass in one horizontal layer and in one vertical layer on the dicing street. The structure of the dicing streets can be seen in Figure 21.

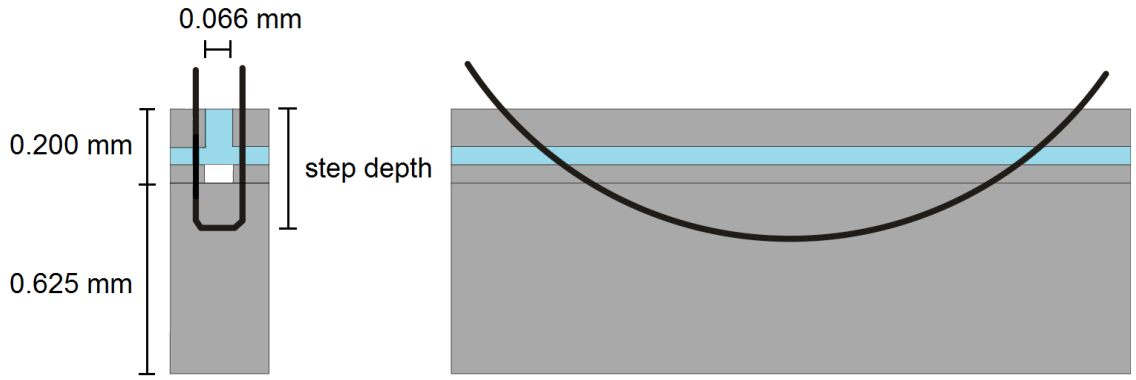

Figure 21 An illustration of the wafer dicing street and wafer dimensions. The black line shows the position of the blade edge during first cut.

The test wafers were mounted on an UV curable dicing tape which has a strong adhesion layer. Different blades were used on Z1 and Z2 spindles. 1st cut blade in the Z1 spindle was a metal bond blade. The blade options for Z2 in the screening DOE were a metal bond blade and an electroformed nickel bond blade. Dressing boards were chosen according to the recommendations of the blade manufacturer. More detailed blade information can be found in Table 2.

Table 2 Blade specifications.

Blades	Bond type	Outer diameter (mm)	Thickness (mm)	Diamond grit size (mesh)	Diamond concentration*
1st cut	Metal bond	58	0.15	1500	50
2nd cut	Nickel bond	56	0.10	1700	60
2nd cut	Metal bond	55	0.10	1500	25

*Concentration refers to the percentage of diamond grit in the abrasive portion of the blade

2.2 Experimental equipment

The equipment needed for conducting the experimental runs and for measuring the output is introduced in this chapter. A fully automatic dicing saw was used for the wafer processing and three different kinds of devices, an optical microscope, a scanning electron microscope and an automated visual inspection device was used to inspect the output.

2.2.1 Fully automatic dicing saw

The dicing saw used in this experiment was a Disco DFD6340 Fully automatic dicing saw (Figure 22). The fully automatic dicing saw can complete the entire dicing process including loading, alignment, dicing, cleaning, drying and unloading altogether automatically. It is a dual spindle dicing saw with an integrated cleaning station. The cleaning mechanism includes an atomizing nozzle which makes the cleaning process effective. [13]

Figure 22 Disco DFD6340 fully automatic dicing saw [13].

The operation flow of the dicing saw can be seen in Figure 23. The mounted wafers are moved by the lower arm from the cassette to the pre-alignment stage and then to the chuck table where the dicing is performed. After finishing the dicing the upper arm moves the work piece to the spinner table for cleaning and drying processes. Finally the work piece is brought back to the cassette. [13]

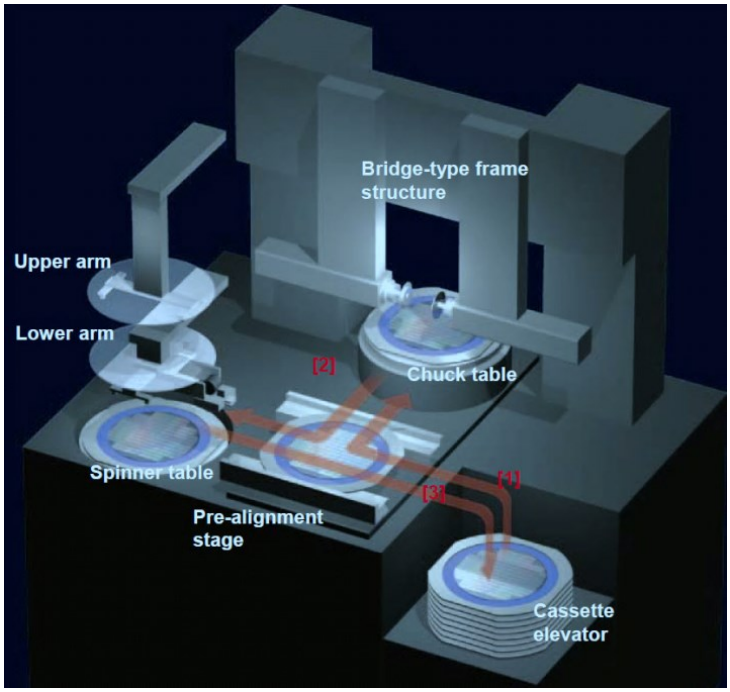

Figure 23 The operation flow of a fully automatic dicing saw. [13]

2.2.2 Optical microscope

An optical microscope can be used for a quick examination of defects, debris, fractures or other abnormality on the element surfaces. High magnification objectives are useful for detecting small deflections even in the magnitude of a few micrometers. An optical microscope has a fairly limited depth of focus which is notable especially at high magnifications. Optical microscopy can utilize either bright field or dark field illumination. In bright field the objects parallel with the optical axis of the microscope are seen as bright areas and inclinations are seen as darker areas. Dark field illumination works in the opposite way so the rays reflected at an angle to the microscope axis are collected and therefore are seen as bright areas. [33]

In this research the optical microscope used was a Nikon Eclipse L200N with NIS-elements software. The microscope was used for examining the front side and back side chipping of the diced elements and to inspect the surface quality of the dicing surface. Bright field illumination was suitable for observing these kinds of dicing defects. NIS-elements software enabled taking pictures of the dies with different magnifications and manual measurement of dimensions and angles.

2.2.3 Scanning electron microscope

A scanning electron microscope (SEM) provides a much greater magnification and depth of focus compared to an optical microscope. SEM is a useful tool for inspecting MEMS devices because in addition to high magnifications it gives the opportunity to tilt and rotate the sample piece to get specific viewing angles. With SEM it is possible to detect features down to the nanometer scale. The sample for a SEM inspection sometimes needs to be coated with a thin conductive film to increase the quality of the image. The sample is placed in a vacuum chamber during the imaging. SEM can also be used to determine the material composition of the sample by using energy dispersive x-ray spectroscopy (EDX). [33] The SEM used in this study was a Hitachi SU8030 shown in Figure 24. The microscope was used for taking high magnification pictures of the blade edge surfaces to inspect the wear of the blades.

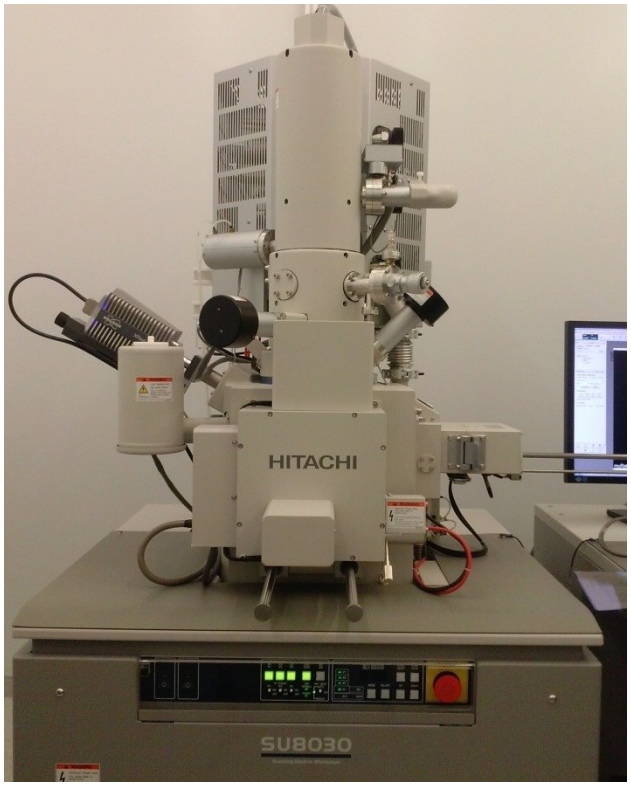

Figure 24 Hitachi SU8030 Scanning Electron Microscope.

2.2.4 Automated visual inspection device

Automated visual inspection (AVI) is an image processing technique used in production line automation to control quality. Visual inspection devices are installed in the fabrication, assembly and testing processes to improve the yield rate and to reduce manufacturing costs. The inspection process can be designed to measure characteristics such as surface quality and geometric dimensions. The computer technology of AVI includes pattern recognition, image processing and artificial intelligence which enable real time and continuous inspections. There are several image processing and classification techniques for AVI such as projection method and filter-based method. AVI can also provide statistical information that can be used for analyzing the manufacturing process. [34]

The AVI device used in this research consists of a probing platform, a camera, optics and different kinds of light sources. Bright light, background light and infrared light are used in the photos to bring out different kinds of defects. Dicing defects related to the geometry of the die are most easily recognizable with the background light whereas surface quality defects are detected with bright light or with a combination of bright light and infrared light. The resolution of the camera is approximately 3 μm.

In this research AVI is used for measuring the size of back side chipping. The experiment wafers are run through AVI after dicing. The wafers are turned upside down so that the back side of the wafers can be inspected with AVI. Back side chipping of each die is criticized by measuring the biggest chip size on each of the die edges and calculating their sum. AVI inspects the whole wafer one die at a time and records the data. Upper picture in Figure 25 shows how the back side of the wafer looks like when arriving to AVI. Top, bottom, left and right edges of the die backside are illustrated in the lower picture of Figure 25.

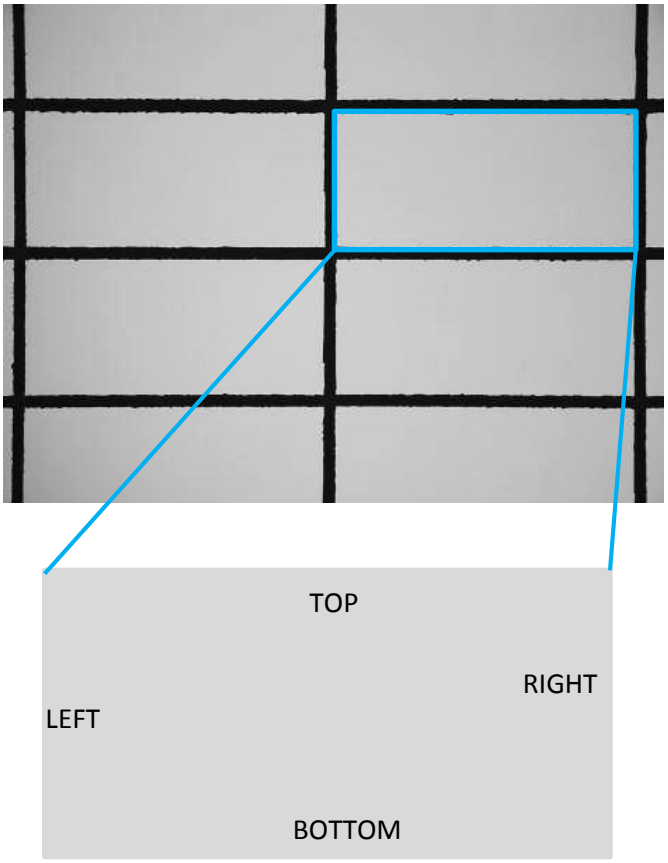

Figure 25 The back side chipping measurement on AVI device.

The AVI program that was used for this experiment is not used in normal production processes. It was made specifically for this experiment to get numerical data for statistical analysis about back side chipping. No measurement systems analysis had been done to this program so the reliability of the data should be reviewed critically. However, the accuracy of the measurement was found good enough for this study because the data was mainly used for comparing the values between the experimental runs.

2.3 Conducting the experiment

The process characterization was done in this research by Design of Experiments. The following chapters introduce the principle of this statistical method and describe how the screening and optimization DOEs were conducted.

2.3.1 A Design of Experiments

A Design of Experiments (DOE) is a process of planning, designing and analyzing an experiment in a way that makes it possible to draw valid conclusions effectively from the results. The principle is to implement statistical methods into the experimental design methodology in order to get statistically sound conclusions. The information gained from a properly planned, executed and analyzed experiment can be used to improve a manufacturing process. [35]

Understanding the manufacturing process closely is essential for utilizing a DOE. A process is an action where inputs are turned into outputs. Inputs are factors or process variables that can be changed in the process and outputs are characteristics of the final product (Figure 26). The purpose of a DOE is to make changes to the input and observe the corresponding changes in the output. Some input variables can be controlled but some of them are hard or almost impossible to control during normal production conditions. Uncontrollable variables are responsible for variability and product performance inconsistency. [35]

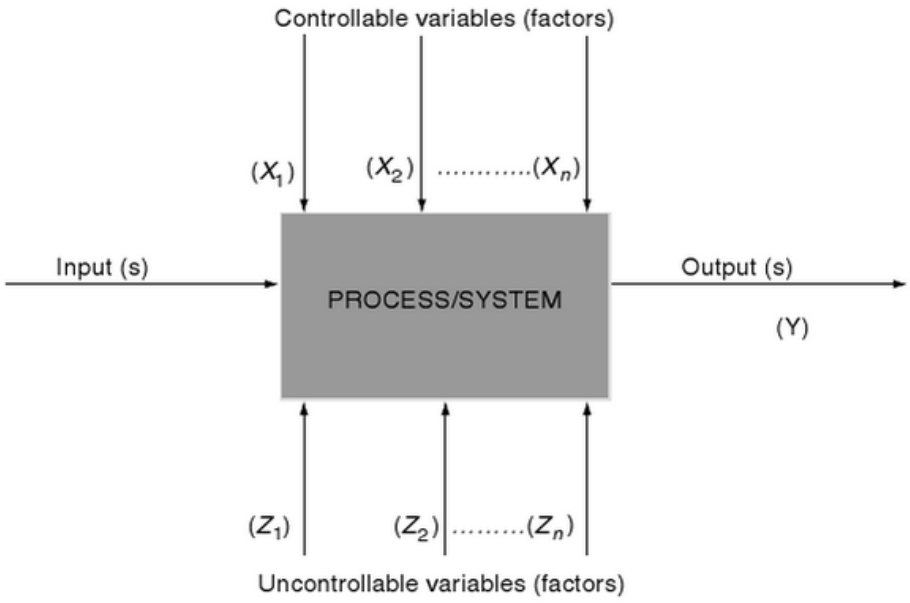

Figure 26 A DOE model of process inputs and outputs. [35]

A Design of Experiments can be either a full or fractional factorial design at two or three-levels. Factorial designs enable the experimenter to study the joint effect of the process parameters on the response. This study concentrates on full factorial two levels design. A full factorial design covers all possible combinations of levels for all factors. The total number of experimental runs in a two level design is determined according to Equation (3).

$$total\ number\ of\ runs = 2^k \tag{3}$$

where *k = number of factors*

A full factorial two level design is usually practical in the early stages of experimental work when k is less than or equal to 4. The assumption that has to be made for factors at two levels is that the response is approximately linear between the chosen factors. A fractional factorial design means that only a fraction of the full factorial design will be run. This allows studying the main effects and low level interaction effects with a minimum number of experimental runs when it can be assumed that certain higher order interactions are not relevant. [35]

Screening and optimization are different kinds of DOE methods and they are commonly used in different phases of a study. Screening DOEs are used to limit a large number of process variables. The meaning is to identify important process parameters which have the most significant impact on the process output. When the key parameters are identified it is possible to do more specific experimentation using chosen parameters and to understand the nature of interactions between them. [35] Optimization is a more specific DOE and is done after a screening design. The most important factors are already identified and the experimental region will be positioned so that it presumably contains the optimal point. [36]

A DOE procedure can be basically divided into four phases which are planning, designing, conducting and analyzing phase as visualized in Figure 27. Planning phase starts with recognizing the problem and deciding the objective of the experiment. The response needs to be defined so that it is clear what kind of outcome is wanted from the experiment. The selection of process variables is an important stage of the DOE procedure because if some

relevant factors are left out of the experiment it will not be as accurate and beneficial as it could be. The process variables and their levels are chosen based on engineering knowledge, previous data, cause-and-effect analysis or for example brainstorming. [35]

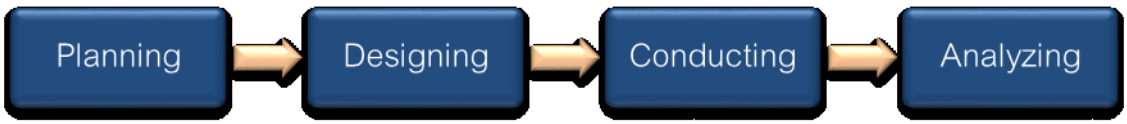

Figure 27 The four phases of a Design of Experiments procedure.

Designing phase consists of selecting an approach for how the experiment will be statistically analyzed. A classical approach advocated by Ronald Fisher, an orthogonal array approach advocated by Genichi Taguchi and variables search approach by Dorian Shainin are examples of different kinds of statistical analysis. A design matrix shows the experimental runs with the settings of factors at different levels and the order of runs. Next phase is the conducting phase where the experiment is carried out and the results are gathered. Monitoring the experimental trials and collecting the response values systematically and reliably is essential. The final phase is to analyze and interpret the results. Final conclusions and suggestions for further improvement are made based on the analysis. [35]

Randomization and replication are methods that help to reduce the effect of experimental bias. By randomizing the experiment it is more likely that every level of factors have an equal chance of being affected by noise factors. The goal is to average out the effect of noise factors that may or may not be present in the process. Replication means running an entire experiment or a part of it more than once. It allows obtaining an estimate of the experimental error and more precise estimate of the factor or interaction effect. If no replicas are used the conclusions about the effects may not be valid. The downside of replication is that it increases significantly the number of runs and the time needed to carry out the experiment. [35]

2.3.2 Screening DOE

Planning of the DOE started with deciding the input and output of the process. Inputs and outputs that were finally chosen for the screening doe are shown in Figure 28

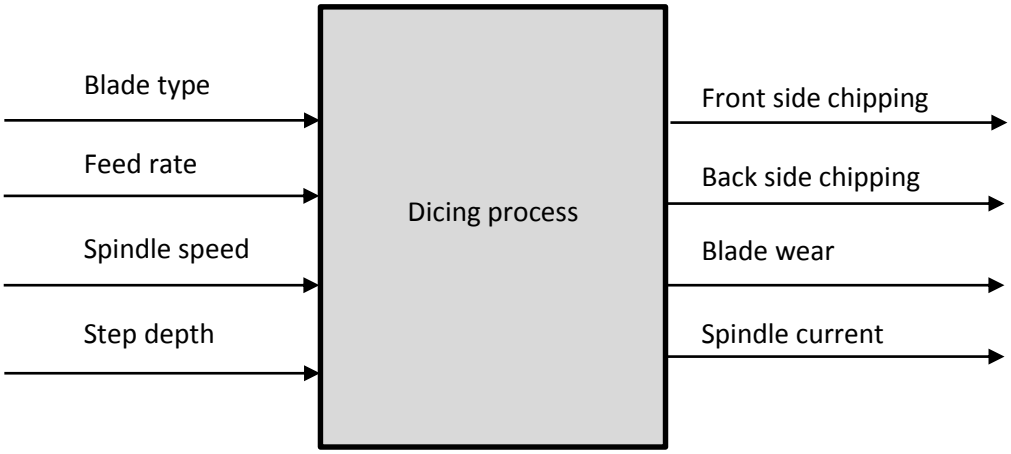

Figure 28 Screening DOE inputs and outputs.

Choosing the inputs was not completely straightforward because there were countless factors that could possibly affect the process. The most relevant factors from our point of view were listed at first and then narrowed down to make a reasonable size Design of Experiments. All the suggested parameters were cut order, mounting tape, blade type, feed rate, spindle speed, and cut depth. The process is a step cut dicing process so the blade and spindle speed can both be separately specified for each cut. This increases the number of available parameters. Cut order describes which channel is cut first. It can have an impact on the outcome especially if the die geometry is not symmetrical. Cut order were chosen to be left out of the DOE because previous trials at MFI had shown that it did not have a big significance to back side or front side chipping. Mounting tape was also left out because there was only one suitable tape choice available for this product. Ordering alternative tapes would have not been possible in the given time period. Based on this reasoning the input parameters for the screening DOE were defined as blade type, feed rate, spindle speed and cut depth.

The factor levels were the next things to be determined. Two levels were defined for each factor. Blade types for the second cut were chosen purely based on manufacturer

recommendations which were a metal bond blade (MB) and a nickel bond blade (Ni). The blade making the first cut in the step cut process was kept as constant. The purpose was to test different blade types only for the second cut blade because it cuts through the back side of the die and has therefore an effect on back side chipping. Feed rate values were defined based on engineering knowledge and previous trials. The single cut method uses a 4 mm/s feed rate so that were chosen as one of the levels. In order to keep the process through put good enough with the step cut method, feed rate needed to be increased. 7 mm/s were estimated as the highest value for feed rate without a big risk of blade overload and breakage so that were chosen as another level. Spindle speed is commonly around 30 000 and the levels for this trial were chosen to be lower and higher than the standard level. The idea was to get noticeable differences in chipping sizes by choosing spindle speeds far enough from each other.

Cut depth was a factor that got a lot of attention because it was a completely new factor in the process due to the newly introduced step cut method. Only a few trial runs were made prior to this DOE. The structure of the wafer and die were examined closely and it was discussed which cut depth would be the most suitable one in theory. There is a glass layer located in the top part of the die structure which affected the choice of cut depth. The main idea of step cut was to remove the glass layer with the first cut and then cut through bare silicon with the second cut. A cut level that reached just underneath the glass layer was 1/3 of the die thickness (step depth 0.33) so that was chosen as one level. The other cut depth was chosen to be as deep as possible without breakage of the remaining wafer. The idea was that the second blade would have to cut through as little material as possible so the cut depth was chosen to be 3/4 of the die thickness (step depth 0.75). The two levels for each factor are listed in Table 3. Cut depth into tape was always 40 μm.

Table 3 Screening DOE and levels.

Factor	**Levels**	
Blade type	MB	Ni
Step depth	0.33	0.75
Feed rate	4	7
Spindle speed	27 000	35 000

Choosing the outputs were simpler because there were clear targets that needed to be improved in the process. Requirements for the outputs were that they had to be easily inspectable and measurable. Back side and front side chipping were defined as the most important improvement targets for this process so they were chosen as outputs. Also spindle current and blade wear were included as outputs to find out their relation to the process parameters. The aim by monitoring spindle current values was also to get information about blade loading and its cutting ability.

The DOE matrix was created using Minitab. The DOE was a four factor two level full factorial design without replicates. The total number of runs according to Equation (3) was $2^4 = 16$. The screening DOE matrix and all the experimental runs are shown in Table 4.

Table 4 Screening DOE design matrix.

StdOrder	RunOrder	Blade	Step Depth	Feed Rate	Spindle Speed
16	1	Ni	0.75	7	35000
15	2	MB	0.75	7	35000
13	3	MB	0.33	7	35000
8	4	Ni	0.75	7	27000
9	5	MB	0.33	4	35000
7	6	MB	0.75	7	27000
5	7	MB	0.33	7	27000
6	8	Ni	0.33	7	27000
10	9	Ni	0.33	4	35000
2	10	Ni	0.33	4	27000
12	11	Ni	0.75	4	35000
11	12	MB	0.75	4	35000
1	13	MB	0.33	4	27000
4	14	Ni	0.75	4	27000
3	15	MB	0.75	4	27000
14	16	Ni	0.33	7	35000

The conducting phase of the experiment started with executing the screening DOE. The wafers were diced with a DFD6340 Fully Automatic Dicing Saw from Disco which is a dual spindle saw. 16 wafers were diced using the parameter combinations defined for each experimental run in Table 4. The Z1 blade was the same type on each of the runs. Only Z2 blade type was changed in the experiment. The wafers were mounted on tape on a dicing frame. Dressing was performed before dicing with dressing parameters defined by the manufacturer. The same dressing conditions were used for all the 16 wafers and the blades were dressed before each

wafer. The same person operated the dicing machine on each run so that the variability in manual processing would be minimized.

Before starting the dicing process the correct parameters from Table 4 were inserted to the dicing program. The wafers were aligned manually and cut automatically. During cutting the values for spindle current were recorded in the beginning and end of cutting the wafer. Progress of the process was monitored by doing occasional hairline and spindle current checks. The wafers were cleaned in the saw's integrated cleaning station in the end of the process.

The blade wear after cutting one wafer was recorded after finishing the dicing process. For additional information about blade wear, a blade profile inspection was done for all blades. It was done by making a half cut into a bare silicon wafer and by inspecting the kerf cross section. The shape of the kerf indicated how the blade edge had worn during dicing.

Next step was to inspect the front side quality of the wafers. This was done with an optical microscope. The whole wafer surface was observed and 3 to 4 pictures were taken of each of the wafers to represent the average chipping size. The pictures from all of the wafers were compared and they were categorized into groups from 0 to 4 based on their chipping level. 0 meaning no chipping at all and 4 meaning that very large chipping were observed. The categorization was done purely by one person observing the pictures so it did not give any absolute values for the chipping sizes. However, this method was considered accurate enough for this experiment and front side chipping inspections with AVI device would have been more time consuming.

The following step was to observe back side quality. The wafers needed to be flipped upside down for this inspection. The mounting tape was exposed to UV light so that the diced wafer would detach easily. The wafer was then placed upside down on another tape frame and pressed gently against it. The new tape frame had not been exposed to UV light so when the old tape was peeled off of the diced wafer, the elements stack on the new tape. As a result, the back sides of the elements were facing upwards and it was possible to inspect their chipping rate. An optical microscope inspection was made for the backside as well but no categorization was done. The back side chipping measurement was done with the AVI device. AVI inspection was made only for the back side of the wafer because back side chipping was the main issue causing poor die quality. Therefore, more specific data from these defects were

necessary. The wafers were run through an AVI program that inspected and measured values for back side edge chipping as described in Chapter 2.2.4.

After finishing the front side and backside inspections with the optical microscope and AVI for all the 16 wafers the conducting phase of the screening DOE was complete.

2.3.3 Optimization DOE

The optimization DOE design was created after completing the screening DOE. The factors were chosen based on the results of the screening DOE which are represented in Chapter 3.1. Feed rate, Z2 spindle speed and step depth were taken into closer observation by defining new levels for them. The inputs and outputs of the optimization DOE are listed in Figure 29.

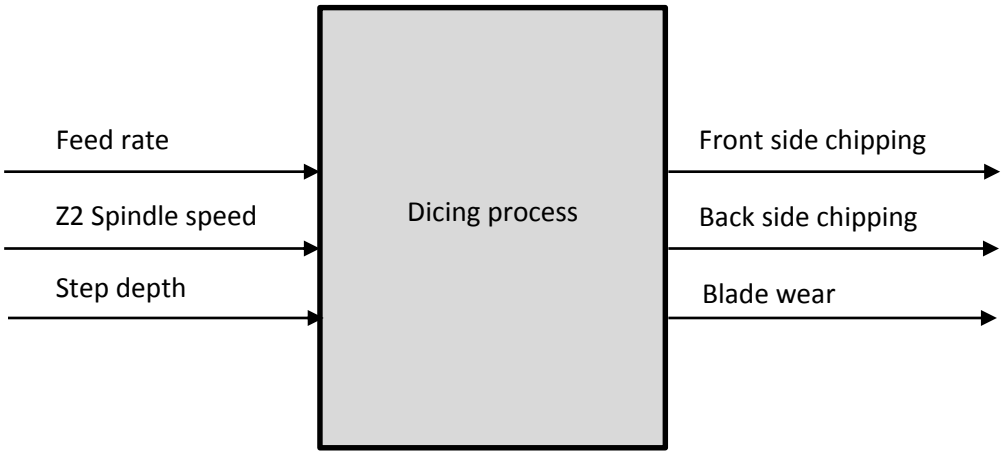

Figure 29 Optimization DOE inputs and outputs.

Feed rates that were chosen for optimization were 6 mm/s and 7 mm/s. 7 mm/s had given good results previously so another level were chosen close to it to narrow down the process window. 7 mm/s was the maximum feed rate recommended by the manufacturer and dicing with 7 mm/s had already resulted in two blade breakages in previous trials so increasing the feed rate above that value was not seen as a good option.

Spindle speed for Z1 was kept constant but spindle speed for Z2 was chosen as a parameter in the optimization DOE to further inspect its impact on back side quality. The object was to

ensure that a lower spindle speed gives constantly better back side quality and if a value close to 27 000 would result in even better quality. 30 000 rpm were chosen as another level for Z2 spindle speed. This is a value that is most commonly used in production processes so there was an interest to study if the value would be suitable for this new step cut process as well.

In the screening DOE a shallower step depth was found to be more beneficial for back side chipping so step depths 0.33 and 0.5 were chosen for the optimization DOE. 0.33 had proven to give good results and 0.5 was in between the two previously studied levels. It was under interest to narrow down the process window and to see whether the impact of step depth was linear. All the chosen factor levels are represented in Table 5.

Table 5 Optimization DOE factors and levels.

Factor	Levels	
Step depth	0.33	0.50
Feed rate	6	7
Z2 Spindle speed	27 000	30 000

Front side shipping, back side chipping and blade wear were chosen as outputs. Spindle current observation was left out of this DOE because it was not seen as a matter that would have given any additional value in this stage.

A three factor two level full factorial design without replicates was created for process optimization. The total number of runs according to Equation (3) was $2^3 = 8$. The DOE design matrix with all the experimental runs are shown in Table 6.

Table 6 Optimization DOE design matrix.

StdOrder	RunOrder	Cut depth	Feed Rate	Z2 Spindle Speed
7	1	0.33	7	30000
6	2	0.50	6	30000
1	3	0.33	6	27000
2	4	0.50	6	27000
4	5	0.50	7	27000
8	6	0.50	7	30000
5	7	0.33	6	30000
3	8	0.33	7	27000

The optimization DOE was conducted in the same way as the screening DOE described in Chapter 2.3.2 but with new combinations of process parameters for each experimental run. The number of experimental runs in the optimization DOE was smaller than in the screening DOE. Similar inspections with the optical microscope and AVI for front side and back side chipping levels were performed.

Additional inspections of blade edge surface, die geometry and cut surface quality were done after finishing the optimization DOE measurements. The blade edge surface was inspected with a SEM. Pictures with magnifications of 500x, 1000x and 2000x were taken of three blades in different stages of the process: before dressing, after dressing and after dicing. The die appearance was inspected by an optical microscope. The sidewalls of a few dies around a wafer were manually inspected with an optical microscope using the NIS-element software. The goal was to check that die dimension and angles were in acceptable limits and if some other abnormalities were present.

3 Results and Discussion

The results and discussion of the screening and optimization DOEs are presented in the first two chapters. The DOE analysis was performed using Minitab and the results are plotted as main effects and interaction plots. The results are divided into four areas by the process outputs: front side chipping, back side chipping, spindle current and blade wear. Summaries of the DOE findings with the optimal parameter choices can be found in the end of each of the chapters. The last two chapters reveal the findings from additional inspections after performing the DOEs including blade edge SEM inspections and observations of die geometry.

3.1 Screening DOE

The raw data for all the chosen outputs of the screening DOE are represented in Table 7. The measured outputs were front side chipping, back side chipping, blade wear during dicing and spindle currents in the beginning and end of dicing a wafer.

Table 7 Screening DOE data.

Run order	Front side chipping	Back side chipping (µm)	Blade wear during dicing (µm)		Spindle current, beginning (A)		Spindle current, end (A)	
			Z1	Z2	Z1	Z2	Z1	Z2
1.	1	147.98	25	0	2.40	1.95	2.20	1.85
2.	1	70.60	28	2	2.35	1.80	2.26	1.78
3.	2	61.19	13	4	2.08	1.95	2.03	1.85
4.	2	100.02	34	0	2.15	1.80	2.00	1.72
5.	1	65.94	11	4	2.15	1.94	2.06	1.80
6.	2	61.75	36	5	2.12	1.60	1.97	1.53
7.	1	55.59	18	11	1.88	1.79	1.85	1.66
8.	2	164.83	23	0	1.86	2.15	1.85	1.93
9.	2	160.43	5	1	2.01	2.48	1.99	2.15
10.	1	159.66	15	0	1.87	2.05	1.84	1.86
11.	1	169.51	22	0	2.33	2.00	2.17	1.85
12.	1	103.77	18	5	2.40	1.79	2.20	1.71
13.	1	83.66	16	6	1.79	1.70	1.77	1.60
14.	1	143.51	28	0	2.14	1.74	1.95	1.66
15.	1	76.36	31	2	2.04	1.60	1.93	1.55
16.	1	193.41	13	0	2.14	2.39	2.12	2.10

The factorial design was analyzed using Minitab. Main effects and interactions plots were drawn for front side chipping, back side chipping, spindle current and blade wear for both Z1 and Z2. The main effects plots give information about which parameters have an effect on the response and which parameter level is preferable. Interaction plots show in which way the parameters are dependent on each other.

Blade breakages occurred during experimental runs number 2 and 4 blade. To find out if the breakages happened due to unsuitable parameter combinations or due to uncontrollable factors new wafers were diced with the same parameter combinations. Neither of the new runs resulted in blade breakage so the breakages most probably occurred due to uncontrollable factors. Another possibility is that the parameters were right on the edge of the process window and a small variability caused the breakages. Runs number 2 and 4 had both a feed rate of 7 mm/s and step depth 0.75 which might have caused excessive blade loading. The results for runs number 2 and 4 in Table 7 were recorded from the new wafers.

It needs to be taken into account that a large range of uncontrollable variables were also present in this experimental design and it needs to be considered when analyzing the results. It would be an impossible task to eliminate or even recognize all the uncontrollable factors. They might be related for example to previous process steps which might have affected the quality of the test material. It is possible that especially the variability between the test wafers has had some impact on the results. Another thing lowering the reliability of the DOE results is the lack of replicates. Replication was not used in this DOE because the number of experimental runs would have decreased too high. It would not have been possible to carry out such a large experimentation in the given time frame. These experiments were done only with new blades which also might have had an effect on the results. The blade's behavior throughout their life time should be inspected to assure the validity of the results over time.

3.1.1 Front side chipping

Front side chipping was inspected manually with an optical microscope and the wafers were categorized into groups based on the average front side chipping level. Figure 30 shows two examples of wafer front side qualities. The picture on the left shows die edges with really small front side chipping (wafer no. 10) and on the right are die edges with bigger chipping (wafer no. 4). The categorization for front side chipping can be seen in Table 7. An assumption was made

that the blade parameter does not affect front side chipping because only the Z2 blade was changed. Z2 cuts through the back side of the wafer and do not cut the front side.

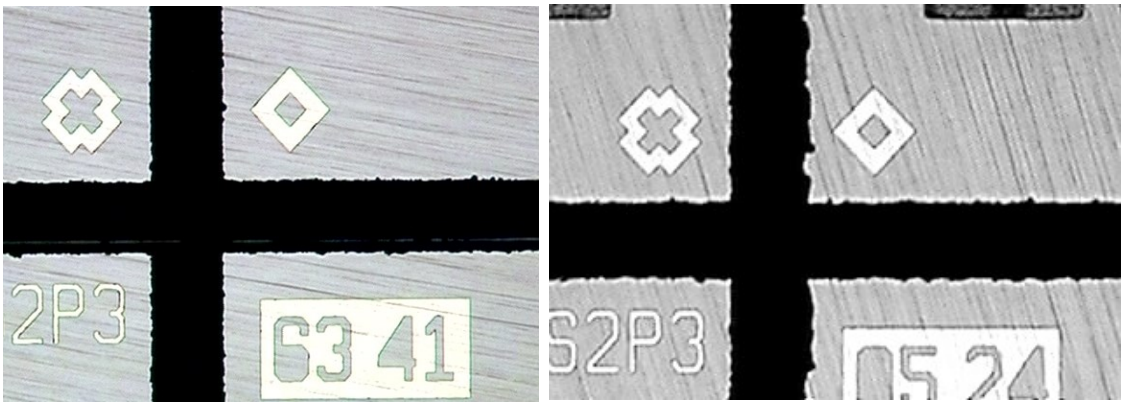

Figure 30 Wafer on the left has less front side chipping than the wafer on the right.

Main effects plot for front side chipping are represented in Figure 31. From the main effects plot it can interpreted that step depth 0.75, feed rate 4 mm/s and spindle speed 35 000 give a lower level of front side chipping.

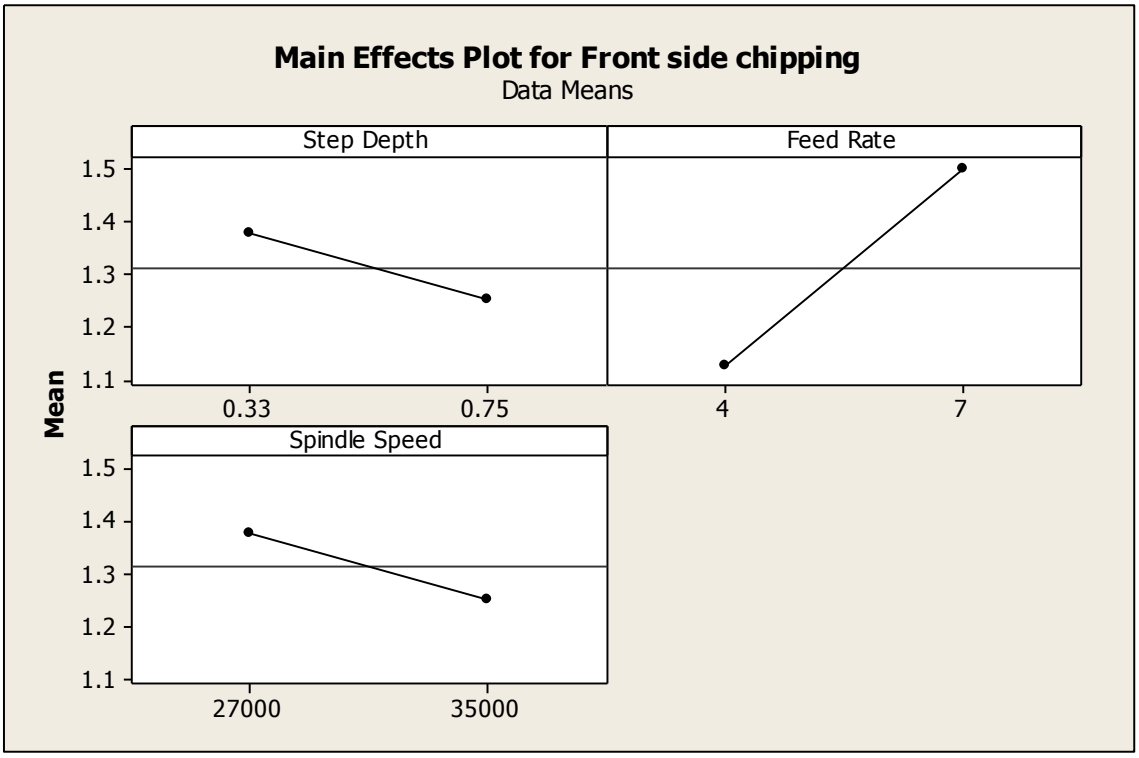

Figure 31 Step depth, feed rate and spindle speed main effects plot for front side chipping.

A deeper cut were beneficial for front side quality and an increased feed rate seemed to cause more chipping on the front side. A deeper cut was better probably because the blade vibrates less when it cuts deeper into the substrate. The reason behind the good results with low feed rate and high spindle speed is that with these parameters a single diamond particle removes a only a small piece of material on each rotation. When every diamond particle removes evenly a little bit of material the particles do not hit the front side of the wafer too hard when the blade moves on which reduces front side chipping.

A research by Shi and Yow [26] had showed that the best front side quality was achieved with a deep step depth and a low spindle speed. Their observation about correct step depth is in line with this research but the observations about spindle speed differ. A lower spindle speed should reduce the impact of diamond grits hitting the wafer surface. It might be that a higher spindle speed is more suitable for MFI's process because of the different behaviour of the glass layer on the dicing street compared to silicon.

From the interaction plots in Figure 32 it can be noticed that spindle speed interacts with step depth and feed rate. With step depth 0.33 spindle speed 27 000 rpm gives a better result but with step depth 0.75 spindle speed 35 000 rpm is preferable. This means when cutting deeper into the substrate a higher spindle speed gives better front side quality probably because a higher spindle speed has the ability to remove more material away from the dicing street. Feed rate 4 mm/s is better for either step depths. With feed rate 4 mm/s spindle speed 27 000 rpm gives a better result but with feed rate 7 mm/s a better choice would be 35 000 rpm. It seems that increasing the feed rate requires also an increase in spindle speed.

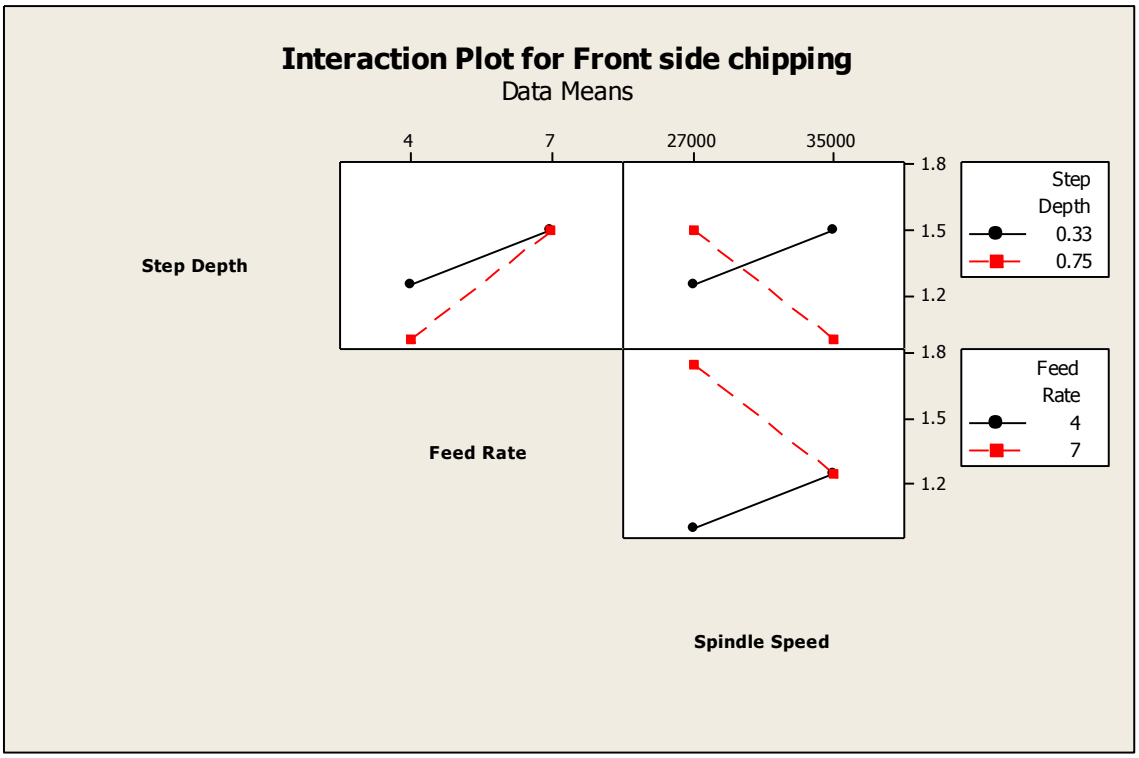

Figure 32 Step depth, feed rate and spindle speed interaction plots for front side chipping.

The results for front side chipping are based on a fairly rough categorization method so their reliability needs to be considered critically. Even so, it was possible to make some conclusions of the analyzed plots. To summarize the interpretations from both the main effects and interaction plots, following observations were made for achieving the best possible front side quality.

- Step depth 0.75
- Feed rate 4 mm/s
- Spindle speed 27 000 rpm with feed rate 4 mm/s or step depth 0.33
  35 000 rpm with feed rate 7 mm/s or step depth 0.75

3.1.2 Back side chipping

Back side chipping was measured by running the wafers through an AVI device and by taking pictures with an optical microscope. AVI measured the biggest top, bottom, left and right edge chip size. Then the sum of these values was calculated and the wafer averages were used to compare the back side qualities between the wafers. The chipping size averages for all the wafers are shown in Table 7. Figure 33 shows two examples of wafer back side qualities. On the left are a picture of die edges with really small back side chipping (wafer no. 3) and on the right are die edges with much larger chipping (wafer no. 11).

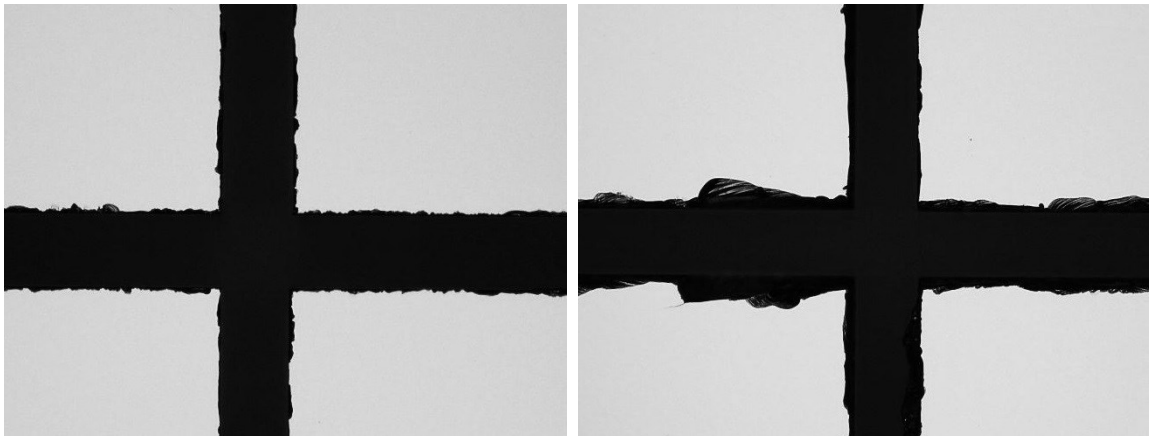

Figure 33 Wafer on the left has less back side chipping than the wafer on the right.

The main effects plots for back side chipping are represented in Figure 34. From the main effects plot it is interpreted that metal bond blade, step depth 0.75, feed rate 7 mm/s and spindle speed 27 000 rpm give a lower level of back side chipping.

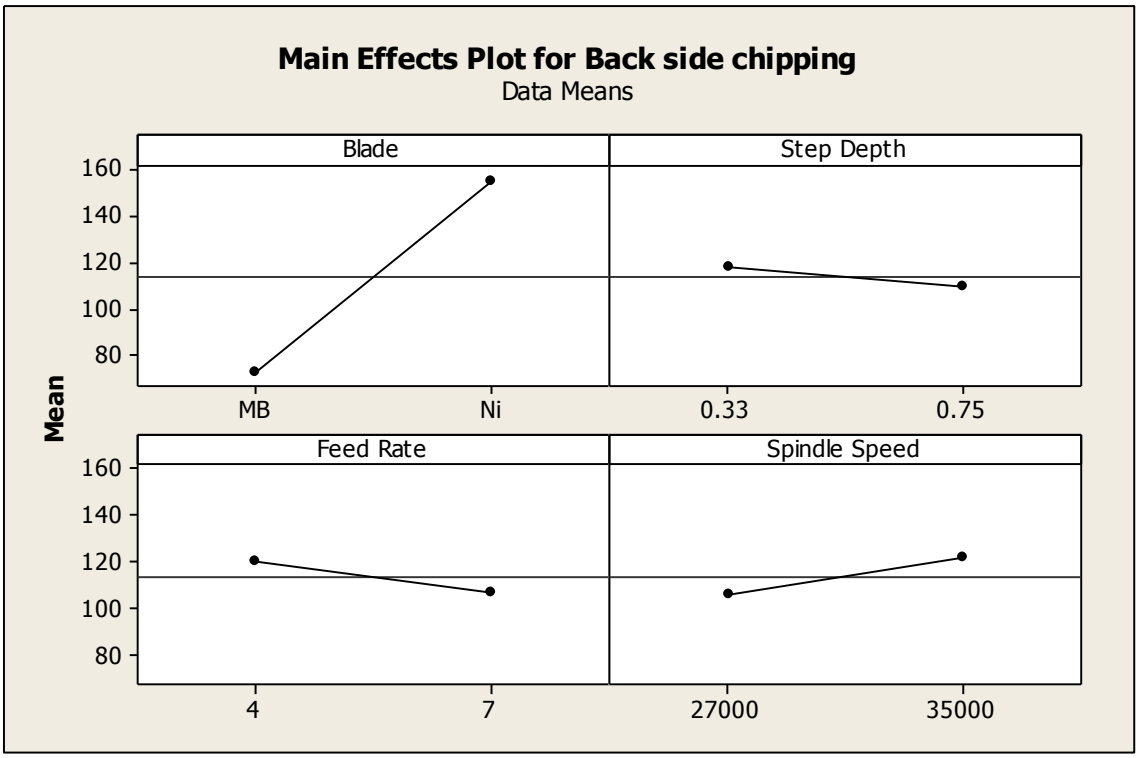

Figure 34 Blade, step depth, feed rate and spindle speed main effects plots for back side chipping.

Metal bond blade induced less back side chipping than nickel bond blade. Nickel bond binder is harder and therefore much less wearing than metal bond binder. In addition to a different bond material the blades had a different diamond grit size and diamond concentration. Metal bond blade had a larger grit size and a lower concentration. The observations are in line with the theory that a lower concentration gives a better cut quality due to more space to accommodate the dicing residue [16]. In addition, in a blade with large grits and lower concentration a single diamond needs to remove a lot of material on each cut. This helps the self-sharpening effect of the blade and keeps the blade load at a low level. A high load and a clogged blade edge results in large back side chipping which was noticed with the nickel bond blade.

The observations about blade wear in Chapter 3.1.3 show that a higher feed rate and a lower spindle speed increases blade wear. A high wear rate means that the blade edge stays in good condition and cuts efficiently through the back side causing less chipping. This is in line with the results gained from the main effects plots for back side chipping. A slow feed rate resulted in poor cut quality. Weisshaus *et al.* observed that this is due to excessive heat generation [18].

Looking at the following interactions plots in Figure 35 it is seen that with a metal bond blade a better result was achieved with step depth 0.33, feed rate 7 mm/s and spindle speed 27 000 rpm. Metal and nickel bond blades showed a difference in the preferable step depth. The explanation might be that the nickel blade gets clogged and causes chipping more easily and therefore it helps if the blade has to cut only through a thin layer of silicon.

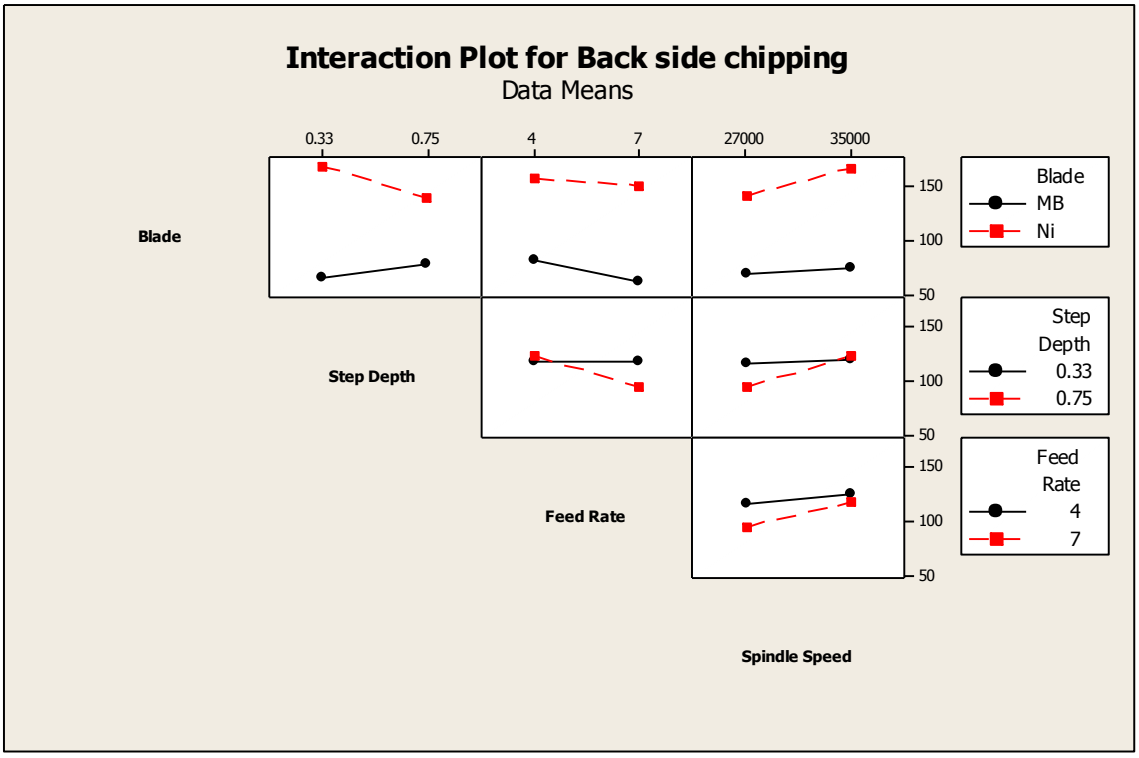

Figure 35 Blade, step depth, feed rate and spindle speed interaction plots for back side chipping.

To summarize the interpretations from both the main effects and interaction plots, following observations were made for achieving the best possible back side quality.

- Blade Metal bond
- Step depth 0.33
- Feed rate 7 mm/s
- Z1 Spindle speed 27 000 rpm

3.1.3 Blade wear

Looking at the main effects plots for Z1 and Z2 blade wear in Figures 36 and 37 it can be seen that the blade wears the least when it has a low feed rate and a high spindle speed and that the wear rate is dependable on the thickness of the layer that it cuts through. Z1 makes the first cut so it wears less when cutting only 0.33 into the wafer and respectively Z2 wears less when cut depth is 0.75 because then it has to cut only through the remaining 0.25 of the wafer thickness.

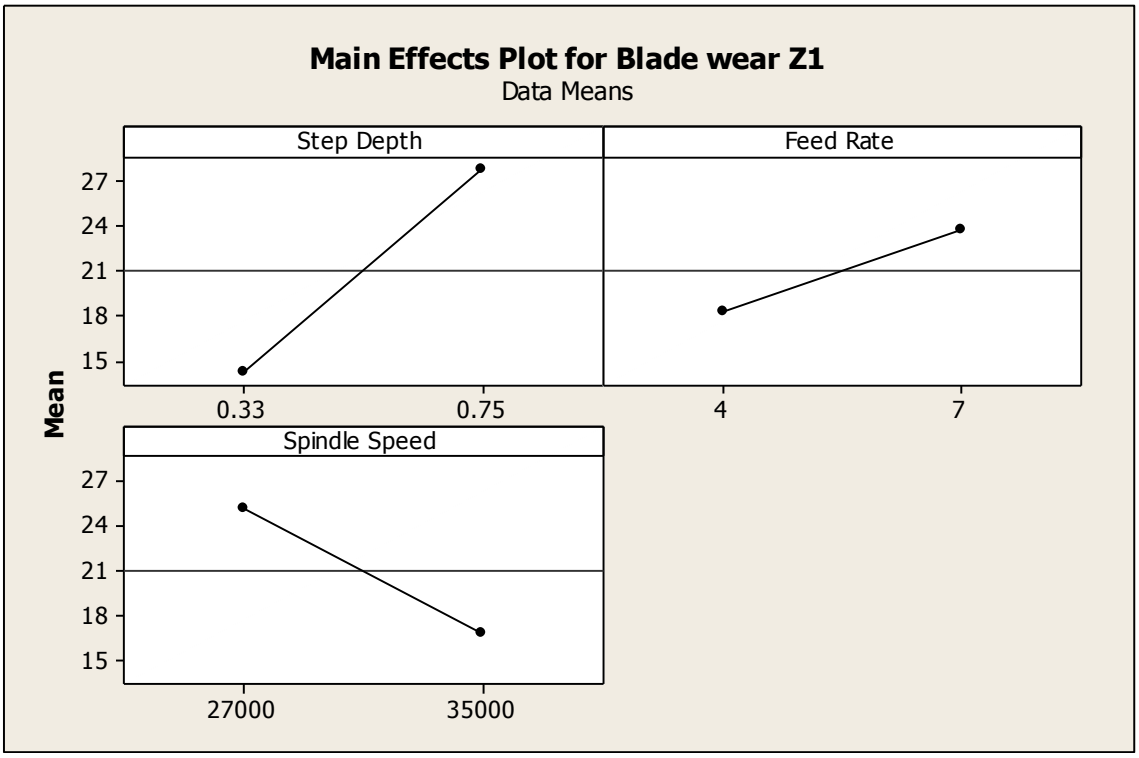

Figure 36 Step depth, feed rate and spindle speed main effects plots for Z1 blade wear.

There was a big difference in the wear rate of the metal bond blade and nickel bond blade. This means that it would be beneficial to choose a nickel blade if the life time of the blade would be a top priority. However, this was not a critical issue in this study so the blade choice was made based on other results. The wear rate of the nickel bond blade was extremely low so it also proves that the blade wear was not enough to keep the blade edge effective enough for cutting.

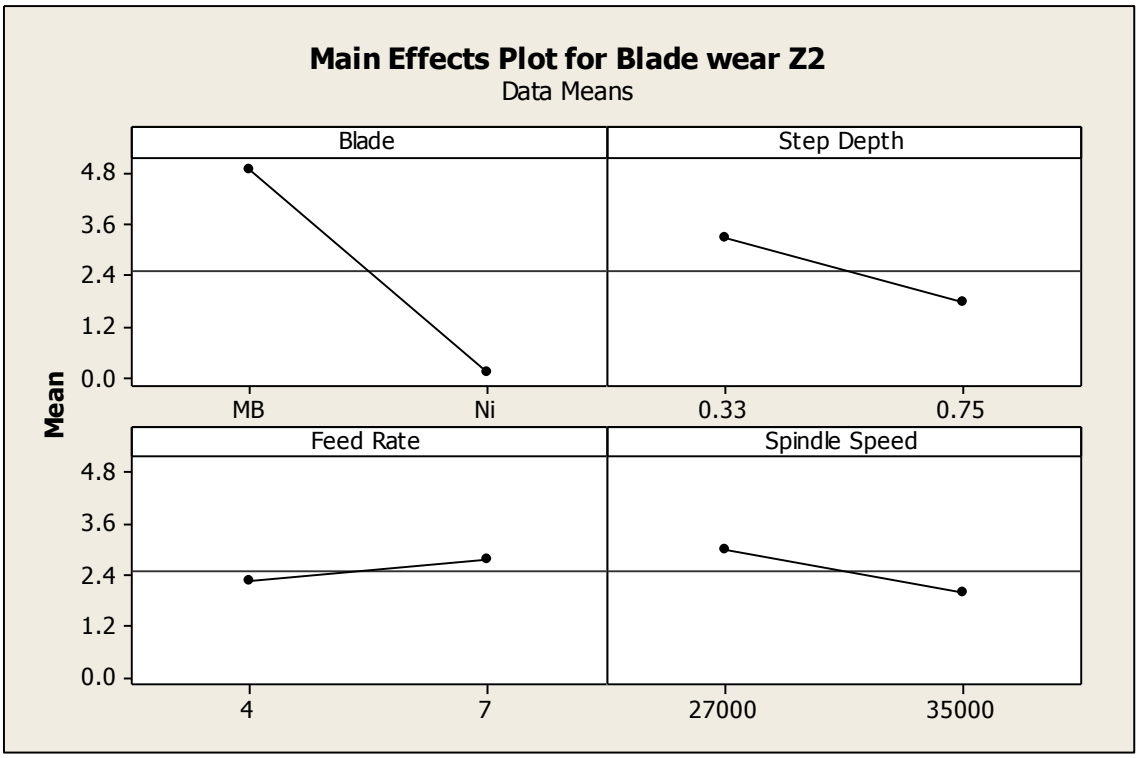

Figure 37 Step depth, feed rate and spindle speed main effects plots for Z2 blade wear.

Pictures of blade cross sections after dicing are shown in Figure 38. When comparing the pictures of the metal bond blade and the nickel bond blade it is clear that the nickel bond blade keeps it shape much better than the metal bond blade. The metal bond blade, with a low diamond concentration, has a more rounded edge because the diamond concentration defines how well the blade edge is able to keep its shape during cutting. The well remained shape of the nickel blade indicates that it probably does not wear a lot which was also noticed from the blade wear values.

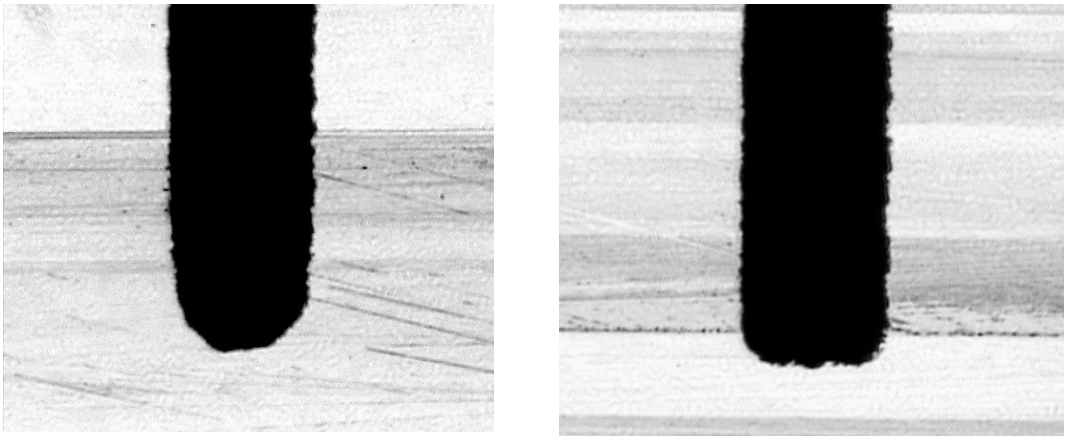

Figure 38 Blade cross section from the metal bond blade (left) and the nickel bond blade (right) after cutting one wafer.

It would be a good thing that the blade edge would keep its shape during cutting but in this case it caused also very large back side chipping. A flat blade edge with a small edge radius would help to eliminate back side chipping caused by the lip effect [16]. With the metal bond blade an adequate conditioning process for the blade edge is therefore more critical. If the lip effect would come up as a problem for the metal bond blade a deeper cut into the tape would also be beneficial.

3.1.4 Spindle current

Spindle current were observed in the beginning and in the end of dicing a wafer. Spindle current values for all 16 wafers at these two points of time are plotted in Figure 39. The most valuable piece of information gained from the spindle current observations was that the spindle current did not rise too high during processing which would have indicated about excessive blade loading. Current values above 3 A would have been too high for this process which is illustrated as a red area in Figure 39. The current was always higher in the beginning of the process than in the end of the process so it decreased during cutting. The dicing saw does not record spindle values so it was not possible to collect continuous data from the current fluctuations. Therefore, the conclusions about blade loading are based only on the two spindle current values recorded for each wafer.

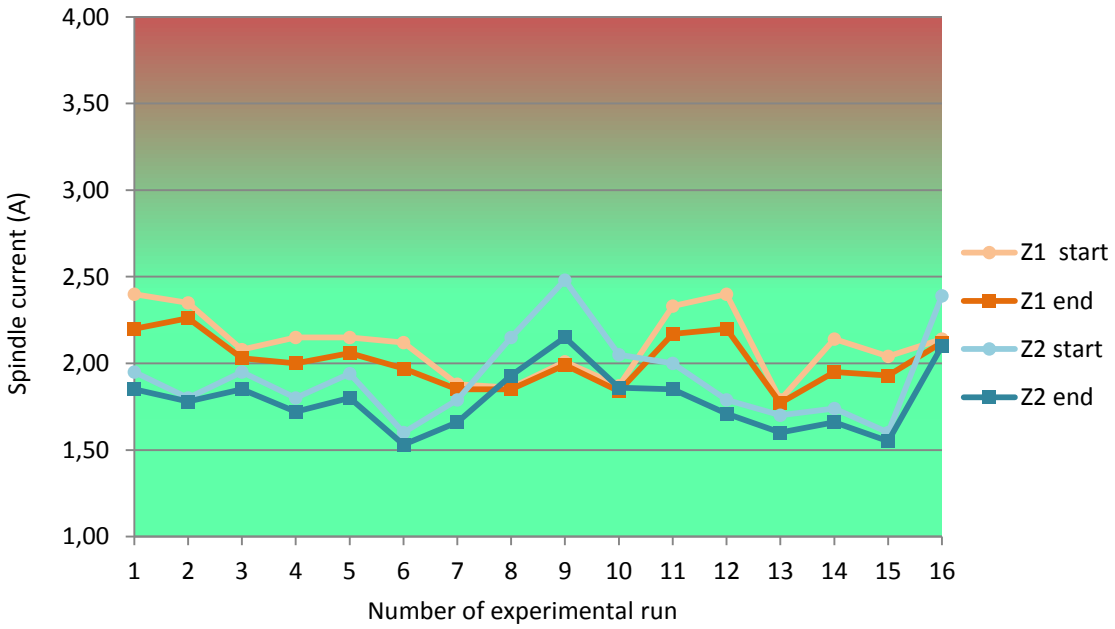

Figure 39 Z1 and Z2 spindle current values for each wafer in the beginning and end of the dicing process.

Figure 40 show the main effect plots for Z1 spindle currents measured in the beginning of the dicing process. The graphs show that a deeper step depth, a higher feed rate and lower spindle speed result in higher spindle current which indicates about higher blade loading.

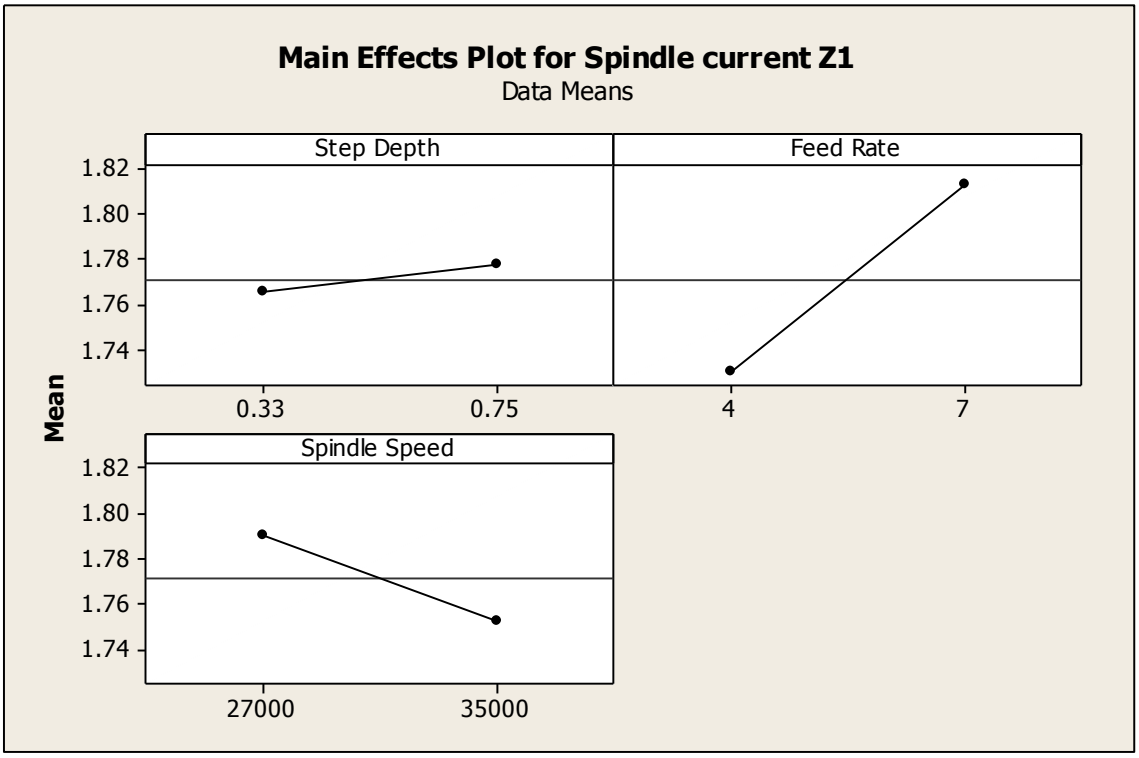

Figure 40 Step depth, feed rate and spindle speed main effects plots for Z1 spindle current.

In the Z2 spindle current plots in Figure 41 it can be seen that also the blade type had an effect on spindle current. With the metal bond blade the current was higher than with nickel blade. This indicates that a higher blade load does not necessarily result in higher level of back side chipping because the metal bond blade gave a better back side quality. An abnormal observation was made from the effect of step depth to Z2 spindle current. Usually cutting through a thicker substrate results in higher load but step depth 0.75, which means there is only a thin layer to cut through, gives a slightly higher spindle current. However, the difference is relatively small.

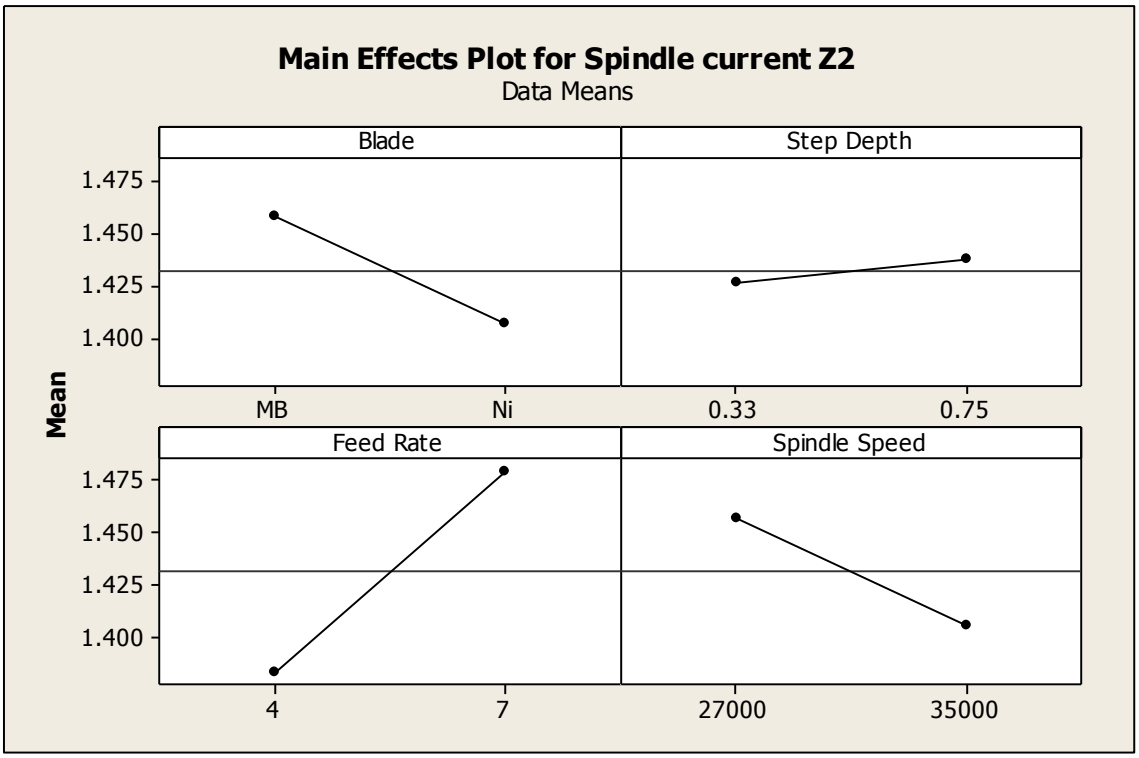

Figure 41 Step depth, feed rate and spindle speed main effects plots for Z2 spindle current.

Luo & Wang [27] and Lei *et al.* [4] had stated that the cutting force increased with high feed rate, high depth of cut and low spindle speed which is the same conclusion that were made from the previous graphs. This would point out that spindle current can be used as an indicator of cutting force. The cutting force can be regulated by changing these parameters according to the desirable directions.

The spindle current decreased during cutting which may be explained by the changes in the blade surface conditions. The surface gets rougher when diamond grits detach from the blade leaving holes behind but becomes more even again when the process moves on. The blade's cutting ability has apparently increased when dicing the first wafer because the current has decreased towards the end of the wafer. Blade surface variations have been proven to result in different cut qualities during dicing in a research by Lin and Cheng [30]. Also variations in blade and wafer surfaces such as diamond grit condition and saw street material affect the cutting force according to Lei *et al. [4].*

The spindle current values (Table 7) were all in a really small range and depended somewhat on the exact time of its registration. So it was not reasonable to make significant conclusions

about preferable parameters purely based on the spindle current values. The results were mainly used to get some idea about the blade load and to verify that the load did not rise exceptionally high with some parameter combination.

The formation of back side chipping is found to correlate with blade torque in a way that above a certain torque limit more back side chipping appears [6]. To see if this kind of relation could be seen in these experiments between spindle current and back side chipping the values were plotted in a scatterplot diagram (Figure 42). The scatterplot shows that the highest back side chipping levels have occurred with the highest spindle currents. Spindle current could therefore possibly be used as an indicator of back side chipping but reasons behind spindle current variations should be inspected more closely. However, an interesting finding about the spindle current observations was that a high feed rate had shown to increase spindle current but simultaneously to reduce back side chipping.

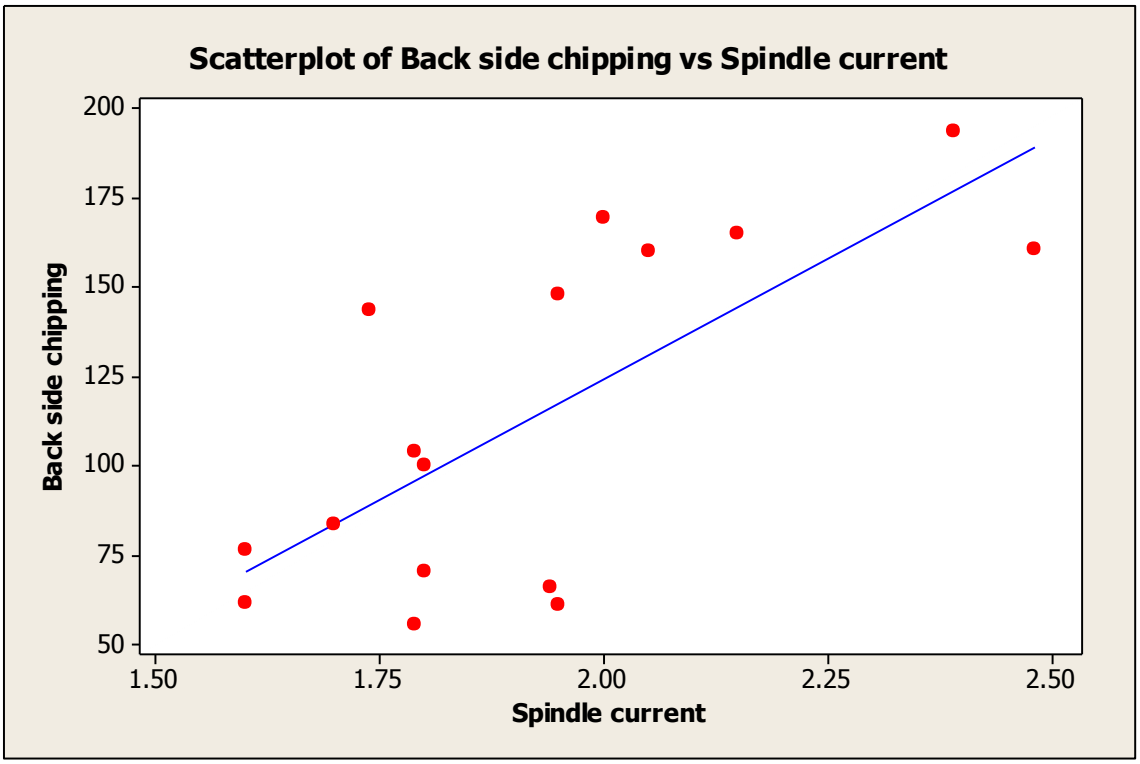

Figure 42 Scatterplot of back side chipping vs spindle current.

3.1.5 Parameter choices after screening

The observations of the effects of input levels to all the outputs are summarized in Table 8. A plus sign indicates a higher value and a minus sign indicates a lower value of the measured output. A lower level is desirable for the front side and back side chipping outputs.

Table 8 Summary of the screening DOE observations.

Parameter	Level	Front side chipping	Back side chipping	Blade wear	Spindle current
Blade	**Metal bond**		-	+	+
	Nickel		+	-	-
Step depth	**0.33**	+	- (with MB blade)	wear increases with cutting thickness	current increases with cutting thickness
	0.75	-	+ (with MB blade)		
Feed rate (mm/s)	**4**	-	+	-	-
	7	+	-	+	+
Spindle speed (rpm)	**27 000**	- (with feed rate 4 or step depth 0.33)	-	+	-
	35 000	- (with feed rate 7 or step depth 0.75)	+	-	+

The results indicate that the correct spindle speed for better front side quality is dependable on feed rate. So when choosing feed rate 7 mm/s because of better back side quality the preferable spindle speed for Z1 is 35 000 rpm. Spindle speed of Z1 were assumed to affect only front side chipping and spindle speed of Z2 only back side chipping.

Back side quality being the top priority the parameter choices were made primarily based on back side chipping results. The chipping size in the original single cut process was approximately four times larger compared to the chipping sizes collected in the screening DOE with step cut. In other words, step cut process showed a clear quality improvement even after the screening DOE.

The parameters that gave the best dicing quality in the screening DOE were

- Blade Metal bond
- Step depth 0.33
- Feed rate 7 mm/s
- Z1 Spindle speed 35 000 rpm
- Z2 Spindle speed 27 000 rpm

3.2 Optimization DOE

The optimization DOE design was made based on the results of the screening DOE. The goal was to take a few parameters into closer observation and fine tune the process. All the raw data that were collected from the optimization DOE trials are represented in Table 9. The factorial design was analyzed using Minitab. Main effects and interactions plots were drawn for back side chipping and blade wear for both Z1 and Z2.

Table 9 Optimization DOE data.

Run order	Back side chipping (μm)	Blade wear after 1 wafer (um)	
		Z1	**Z2**
1.	67.61	17	9
2.	70.65	17	8
3.	63.02	19	8
4.	68.69	16	7
5.	63.68	18	7
6.	59.40	18	4
7.	63.65	12	7
8.	57.33	17	9

The optimization DOE had the same reliability issues that were described for the screening DOE. The reliability and stability of these results could have been increased by using replicates and by investigating the behavior of the blade throughout its life time. Uncontrollable variables can always have an effect on the results as well as the variability in the test material. Replicates were not used in this DOE either because the number of experimental runs would have been too large for the given time frame and the accuracy of the results were expected to be good enough without them. However, the results of this research are based on analyzing a fairly limited amount of data which needs to be taken into account when applying the results into practice.

3.2.1 Front side chipping

Front side chipping was inspected in the optimization DOE and similar categorization was planned to be done as in the screening DOE. When observing the optical microscope pictures there were not any significant differences between the wafers. No quality classification was done because it would not have given any additional value. Figure 43 shows examples of front side qualities of two different wafers. The chipping is really small and in the same scale in both of the pictures. A wafer that is diced with feed rate 6 mm/s is on the left (wafer no. 2) and a 7 mm/s wafer is on the right (wafer no. 5).

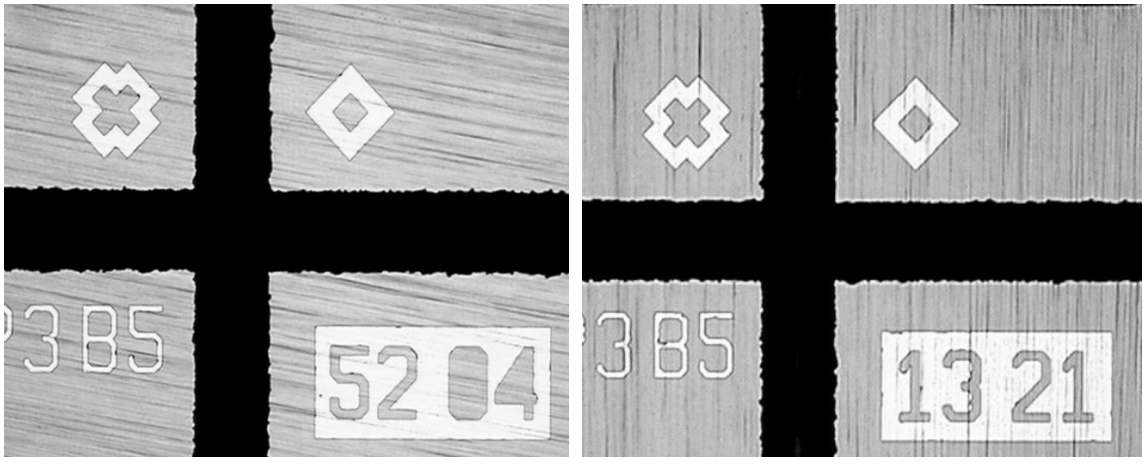

Figure 43 Front side chipping from wafers no 2 and 5.

In the screening DOE a lower feed rate gave better front side quality and the same conclusion can to some extent be drawn from the optimization DOE when comparing the appearance of wafers that are diced either with 7 mm/s or 6 mm/s feed rate. However, all the experimental runs in the optimization DOE gave such a good result for front side chipping that it was not necessary to be taken into closer observation. From now on, the focus was placed purely on back side chipping which had been the major challenge.

3.2.2 Back side chipping

Back side chipping data from the screening and optimization DOEs are plotted in Figure 44. The chipping values of the optimization DOE are relatively low and have a small variability compared to the values of the screening DOE. This proves that the analysis of the screening DOE was done successfully and that optimization verified the correct parameter choices regarding back side chipping.

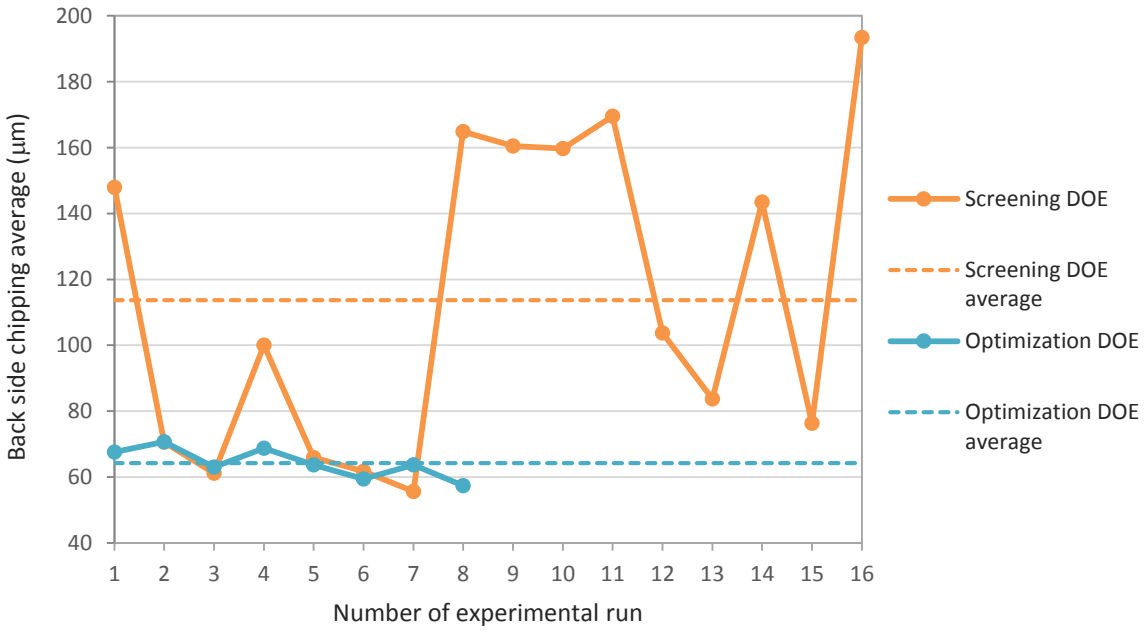

Figure 44 Back side chipping averages for all the experimental runs in the screening and optimization DOEs.

Figure 45 shows two examples of wafer back side qualities. On the left are a picture of die edges with the smallest back side chipping (wafer no. 8) and on the right are die edges with slightly larger chipping (wafer no. 2).

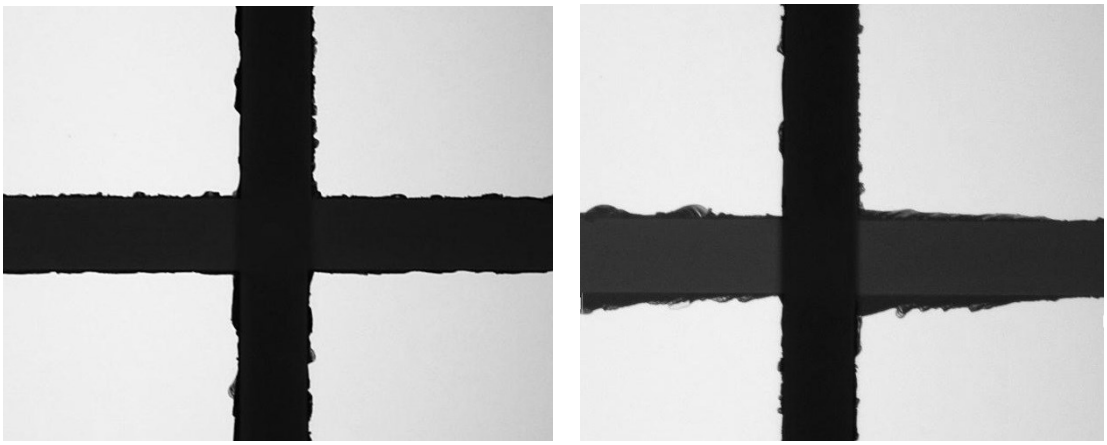

Figure 45 On the left is a picture of a wafer with small back side chipping (wafer no 8) and on the right is slightly larger chipping (wafer no 2).

The main effects plots for back side chipping are represented in Figure 46. They show that the lowest chipping value is achieved with step depth 0.33, feed rate 7 mm/s and Z2 spindle speed 27 000 rpm. These are in line with the screening DOE results for metal bond blade.

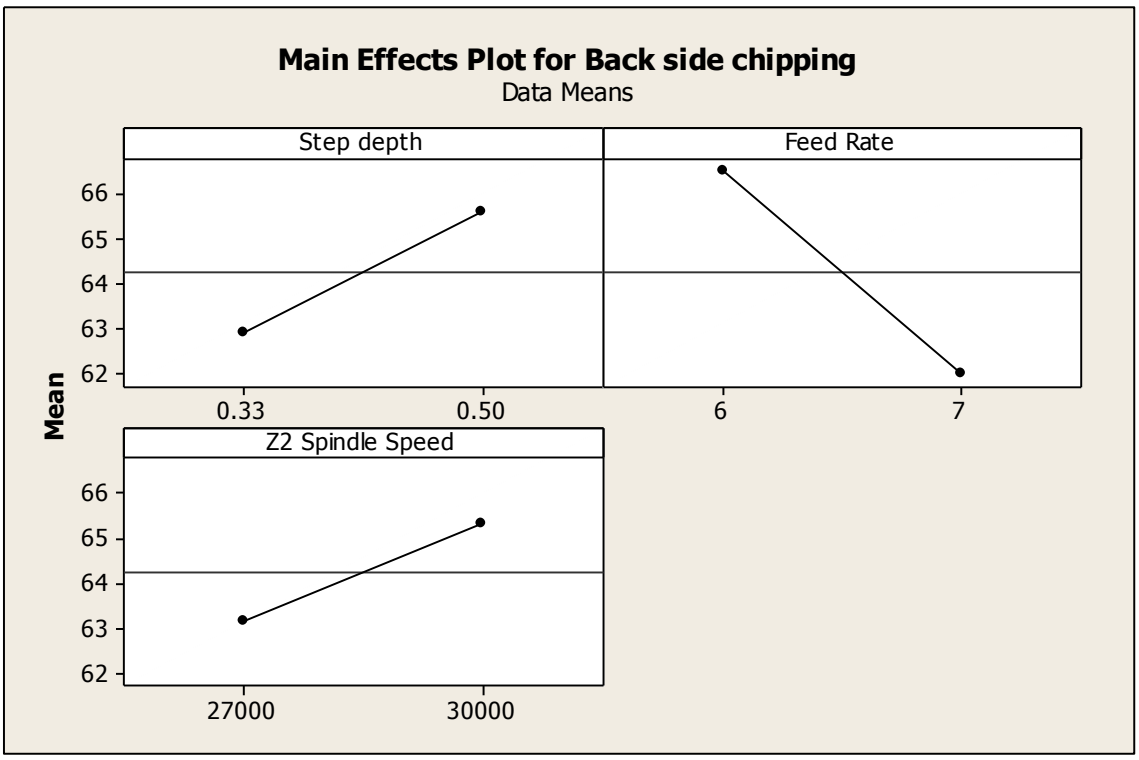

Figure 46 Step depth, feed rate and spindle speed main effects plots for back side chipping.

The observation that can be made about optimal step depth is that a more shallow depth results in less back side chipping. This could be because a shallow first cut leaves a thicker layer of silicon to support the wafer during second cut. The presumption was that a deeper cut would decrease back side chipping because the second blade would have a thinner layer to cut through but these results showed otherwise. Back side chipping is originates from the stresses present on the wafer back surface and high blade load so these results indicate that a thinner layer would be under higher stresses in dicing.

A higher feed rate and a lower spindle speed gave better results in back side chipping in both of the experiments done. A higher feed rate and a lower spindle speed means that the diamond particles of the blade cut off larger quantities of material on each rotation and according the screening DOE results this increases blade wear. A fast wearing blade maintains its cutting ability and prevents it from loading. The diamond particles come loose fast enough and the self-sharpening effect of the blade keeps the back side chipping at minimum.

The interaction plots in Figure 47 indicate a slight interaction between step depth and spindle speed. Step depth 0.33 were chosen based on the main effects plot so spindle speed 27 000 rpm was preferable.

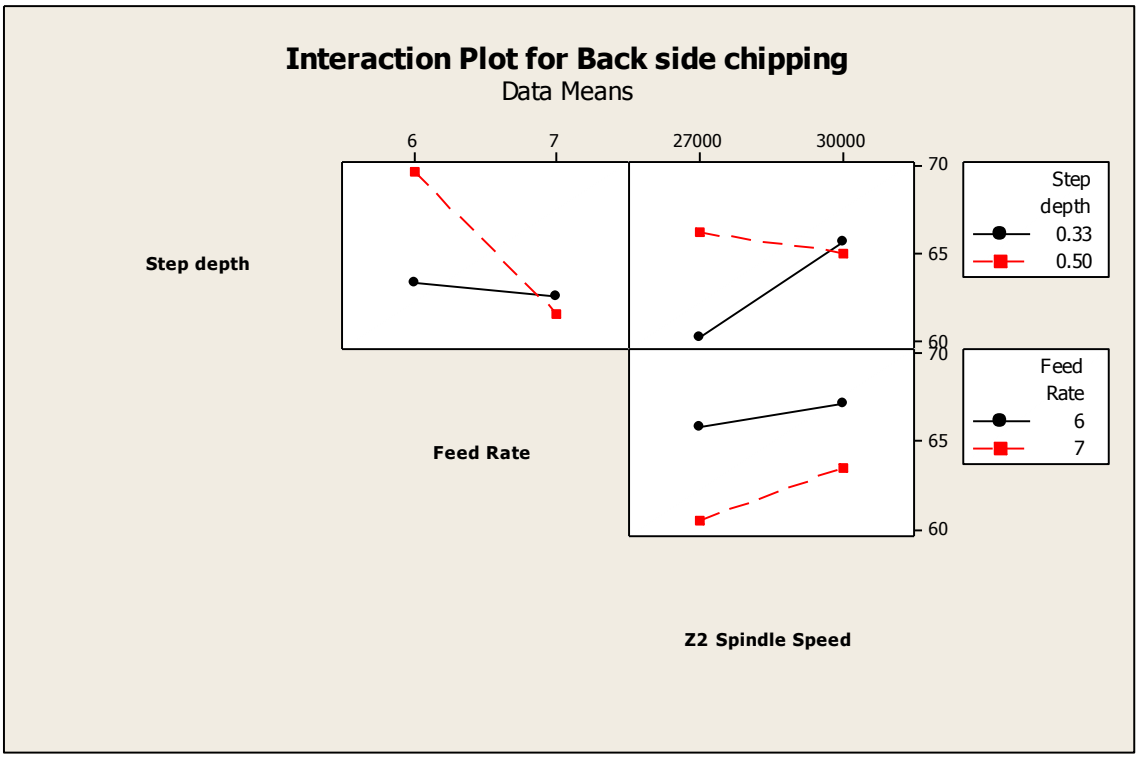

Figure 47 Step depth, feed rate and Z2 spindle speed interaction plots for back side chipping.

To summarize the interpretations from both the main effects and interaction plots, following choices were made for achieving the best back side quality.

- Step depth 0.33
- Feed rate 7 mm/s
- Z2 Spindle speed 27 000 rpm

3.2.3 Blade wear

Main effects plots for blade wear of Z1 and Z2 are represented in Figures 48 and 49. Blade wear was higher when cutting through a thicker substrate layer and with a higher feed rate and a lower spindle speed which is consistent with the screening DOE results. An abnormality was noticed about the Z2 blade wear. The plot for feed rate indicates that a lower feed rate would result in higher blade wear which is inconsistent with other results. Nevertheless, the difference between the two feed rate levels is really small and the differences might have been caused by uncontrollable factors.

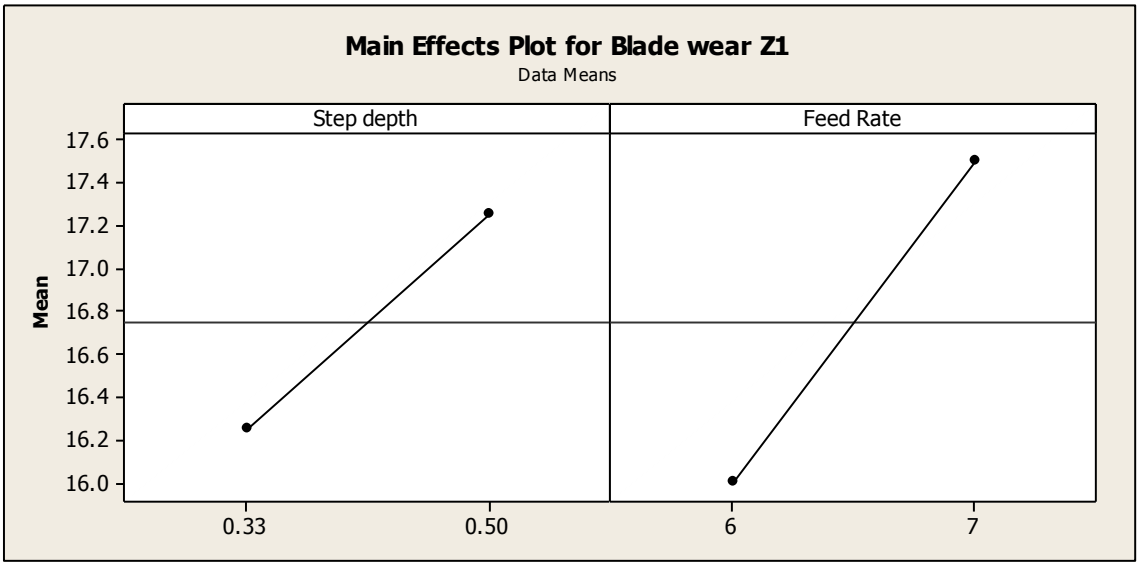

Figure 48 Step depth and feed rate main effects plots for Z1 blade wear.

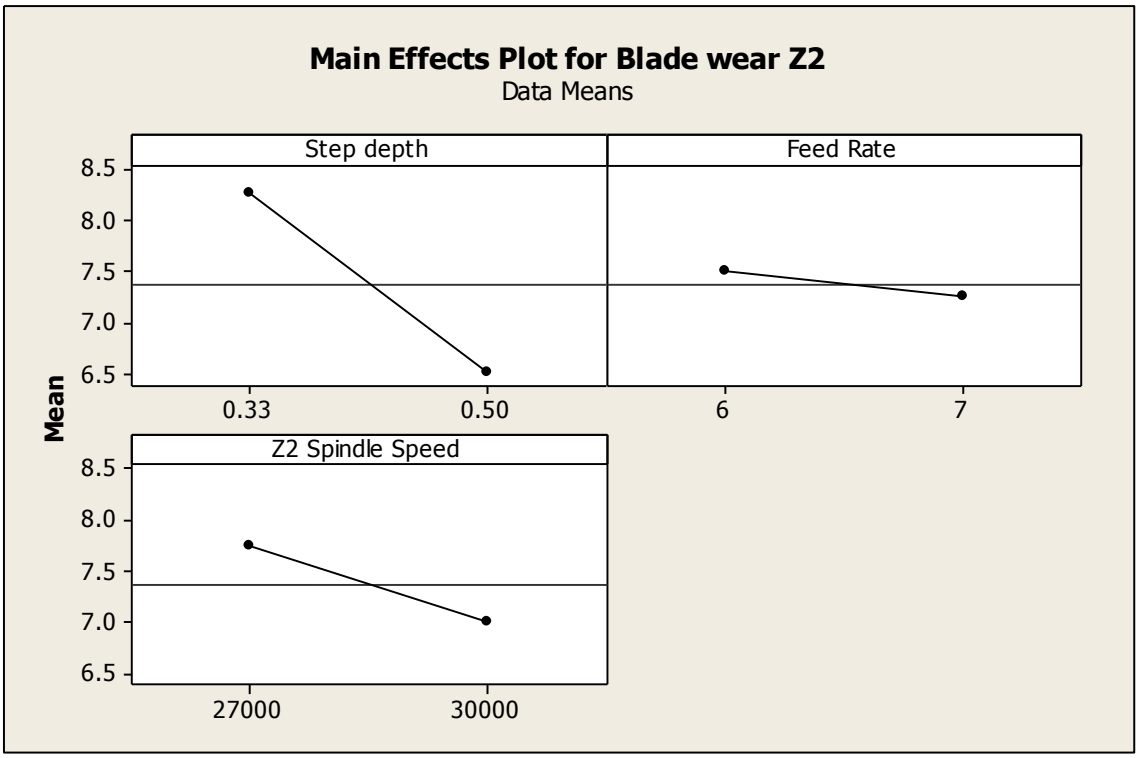

Figure 49 Step depth, feed rate and Z2 spindle speed main effects plots for Z2 blade wear.

3.2.4 Final parameter choices

Front side quality was at such a good level in all the wafers in the optimization DOE that the final process parameter choices were done purely based on back side quality results. Blade wear inspections verified the results of the screening DOE: blade wear increases with the thickness of the substrate layer, with a high feed rate and a low spindle speed.

The end result for the optimized process was based on the analysis of both the screening and optimization DOEs. The final parameter combination chosen for the step cut process was

- Blade Metal bond
- Step depth 0.33
- Feed rate 7 mm/s
- Z1 Spindle speed 35 000 rpm
- Z2 Spindle speed 27 000 rpm

3.3 Blade edge SEM inspection

A blade edge surface inspection was made for the 1st cut metal bond blade that was used for dicing wafer no. 8 in the optimization DOE. Pictures were also taken of similar new blades before dressing and after dressing to be able to compare how the blade edge had changed during dressing and dicing.

Figures 50 and 51 show SEM photos of an undressed blade edge. The diamond grits are visible but they are still mainly embedded in the binder material. The edge shape is flat which was desirable and expected. The surface seems to have a darker layer on top which probably originates from the manufacturing process.

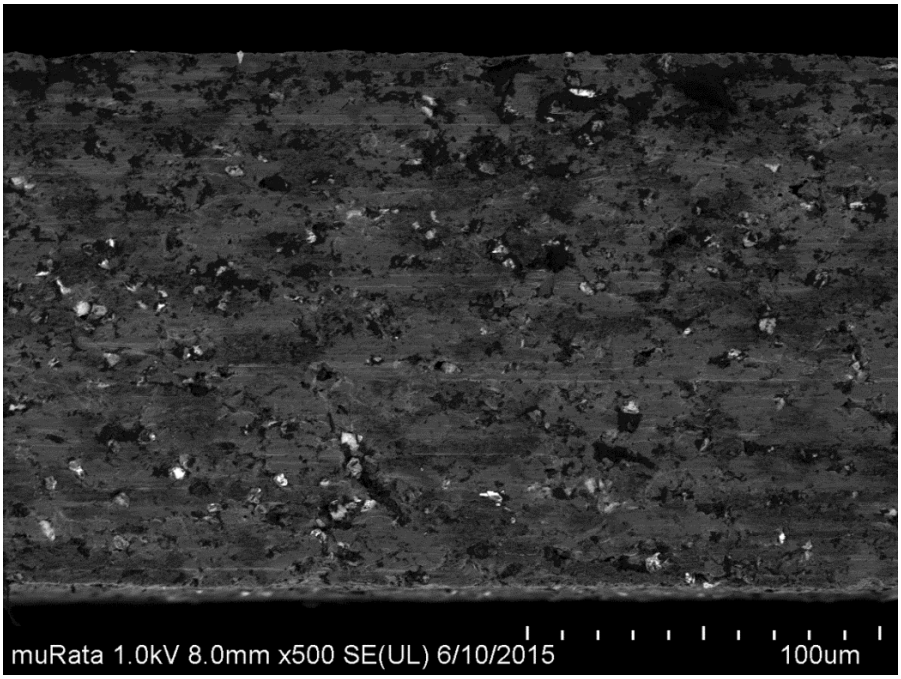

Figure 50 SEM picture of an undressed blade with 500x magnification.

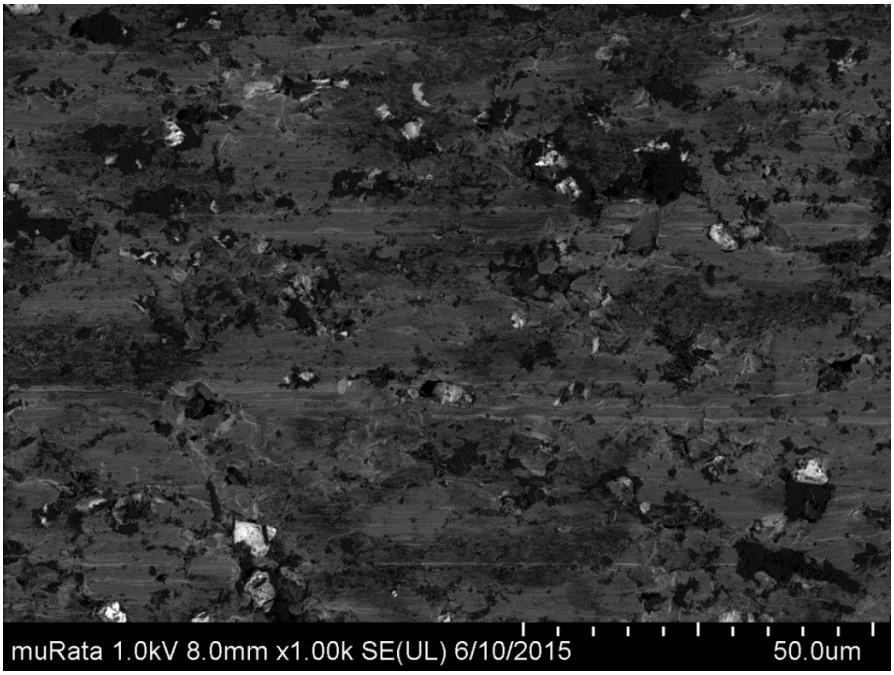

Figure 51 SEM picture of an undressed blade with 1000x magnification.

After dressing the diamond grits are clearly visible and they stand out from the binder material (Figures 52-54). The well exposed diamond particles can especially be seen in the high magnification picture in Figure 54. The blade edge has maintained a good shape with a flat edge and a small edge radius. The small horizontal lines on the surface indicate about abrasive blade wear. The color of the surface is more uniform than in the undressed blade.

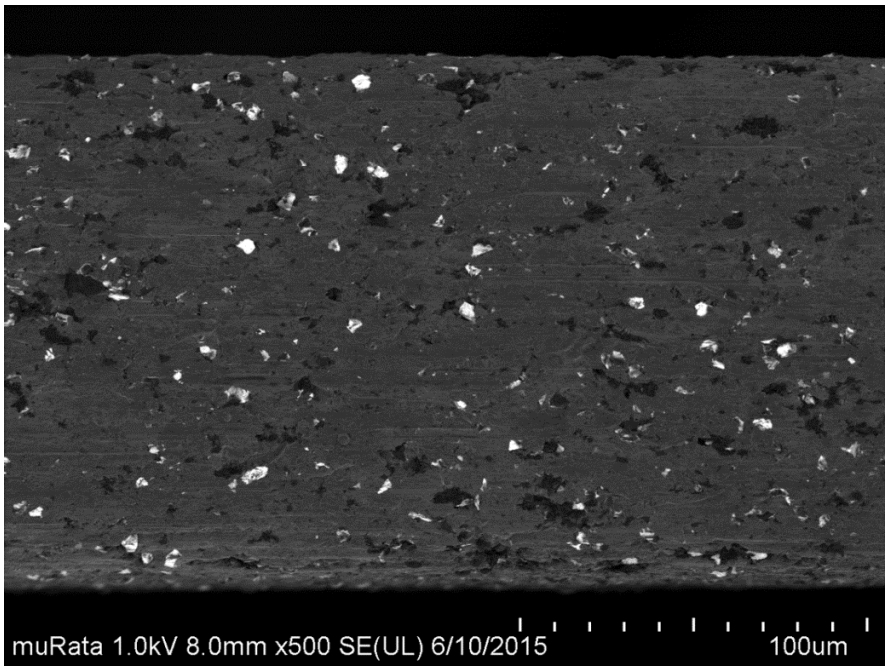

Figure 52 SEM picture of a dressed blade with 500x magnification.

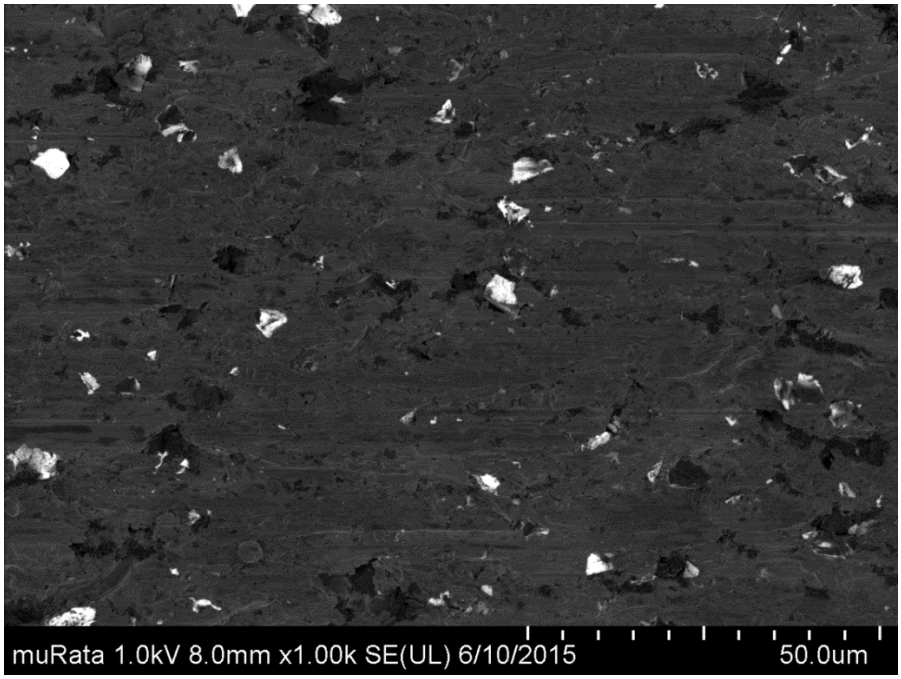

Figure 53 SEM picture of a dressed blade with 1000x magnification.

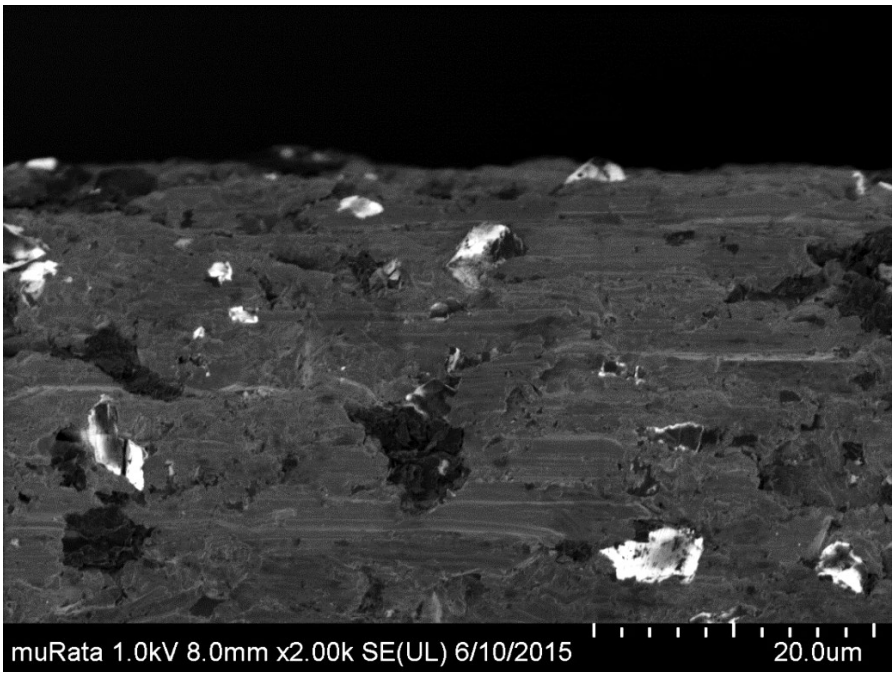

Figure 54 SEM picture of a dressed blade with 2000x magnification.

After dicing, the blade edge had clearly deformed. This can be seen in Figures 55 and 56. There are also more diamond particles exposed than after dressing. The middle part of the blade has worn less than the sides of the blade. Similar results were observed from the blade profile inspection which is introduced in Chapter 3.4 and Figure 59. The diamond grits seem to be equally exposed on the side areas and in the middle so there is no sign of a clogged blade in either of the areas. On the side areas which only cut through silicon can be seen relatively large dimples which were not present in the blade after dressing. The middle part that cuts mainly through glass is more evenly worn and no large dimples were observed.

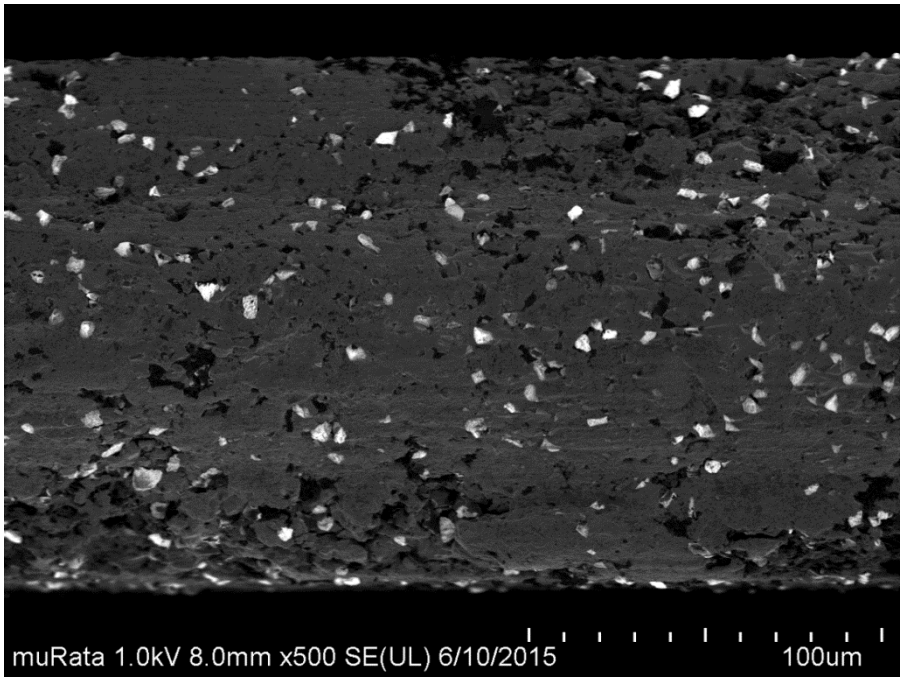

Figure 55 SEM picture of a blade after dicing with 500x magnification.

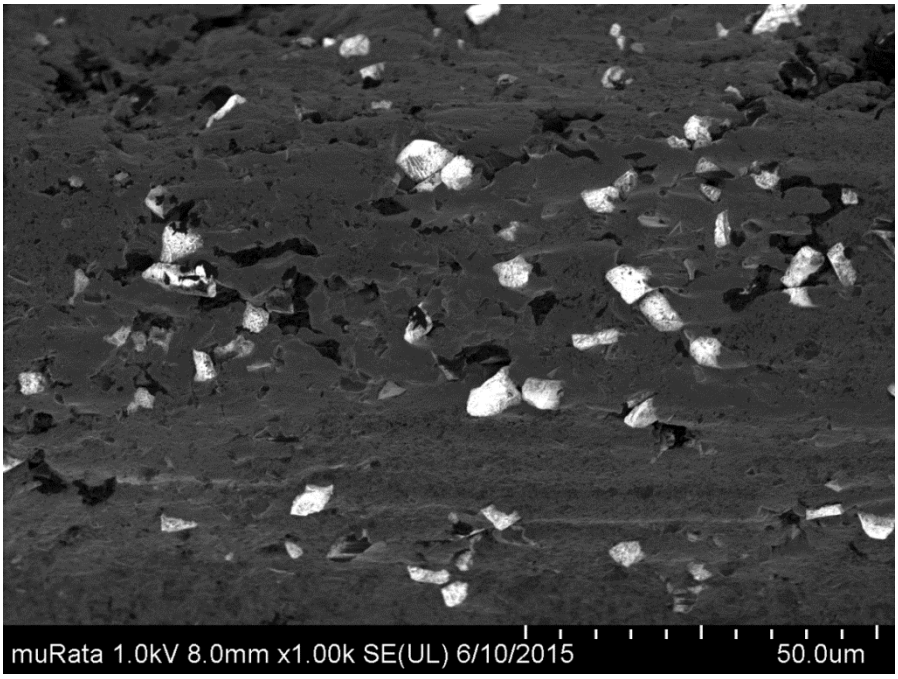

Figure 56 SEM picture of a blade after dicing with 1000x magnification.

The reason behind the decrease in spindle current during dicing can be explained by the observations made from these pictures. Blade cutting ability increases during dicing because the diamond particles become more exposed and blade wears well. An effective blade needs less force to make the cut into the substrate. The diamond particles are still slightly embedded after dressing and the surface is relatively smooth without large dimples which mean the blade is duller than it seems to be after dicing.

The deformed blade edge is caused by the glass layers on the dicing street. The uneven blade wear is due to the different hardness of silicon and glass. The blade matrix should be softer for cutting glass than for cutting silicon. However, there is no sign of a clogged blade edge either in the middle part so the blade seems to be able to cut efficiently enough through this glass layer.

3.4 Additional die geometry observations

An inspection of die geometry and cut surface appearance was performed to check the overall die quality after dicing. The product does not have a functional sidewall so the surface quality is not critical but die geometry and dimensions have to be within specifications. Cut surface quality can however indicate blade loading and cut performance during dicing.

Figure 57 shows the appearance of a typical cut surface of the inspected dies from wafer no. 8. The step cut dies (on the left) were compared to single cut dies (on the right). The divergent blade sawing marks on the die edge were seen on majority of the step cut dies. These marks were observed more closely with an optical microscope and it was verified that the marks did not indicate about incorrect die edge geometry. Similar marks were found on the single cut diced wafers as well so these marks were not caused by the step cut process. The dicing marks are probably formed because the die has moved a bit during dicing.

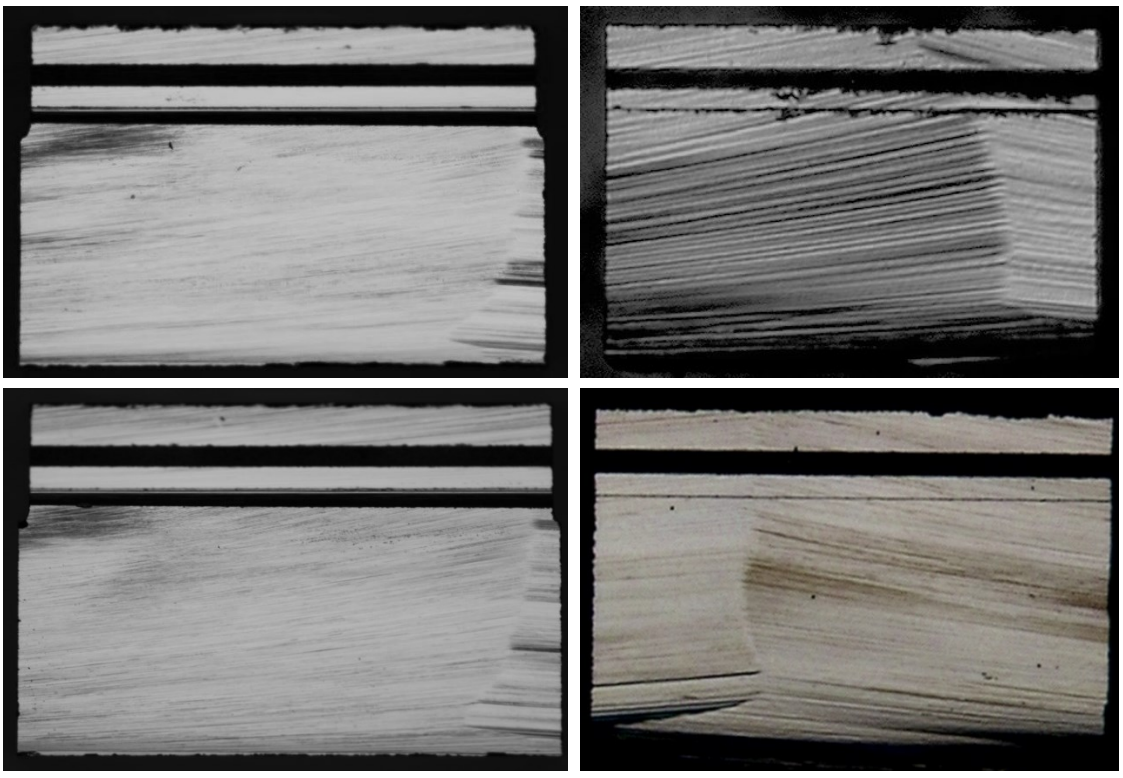

Figure 57 The sidewalls of step cut dies (on the left) and single cut dies (on the right).

The die edge angles that are formed during dicing were inspected manually from a few dies around the wafer. No slanted cuts or lips on the die bottom edge were observed. All the inspected die angles were acceptable.

Step cut leaves a step on the die sidewall because of the different thickness of the first and second cut blade. When observing the diced wafer it was noticed that the dicing kerf had shifted and therefore the die dimensions were slightly changed. The movement of the first cut blade was observed by the shape of the step. Sometimes the step had a groove in the middle and sometimes the sidewall did not have a step at all. An incorrect step shape is shown in Figure 58 (left). Similar kind of step profiles were found repeatedly but not from every dicing kerf.

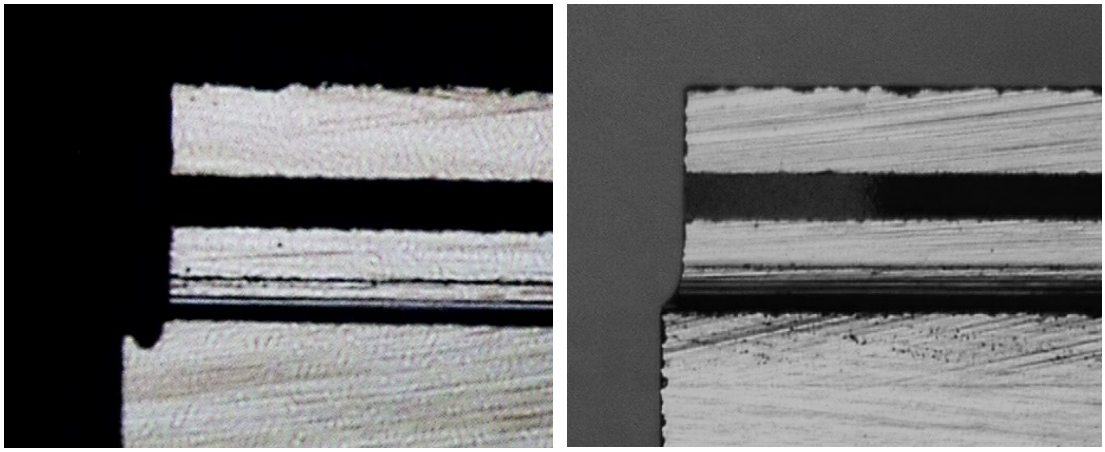

Figure 58 An undesirable (left) and a normal (right) step shape on the die sidewall.

The shape of the first cut groove affects the step shape so an inspection of the first cut blade edge profiles was performed. Pictures of blade profiles after dicing each wafer from the optimization DOE are shown in Figure 59. The same kind of curved shape can be more or less found in all of the blades. The blades had worn more from the outside edges than from the middle. The less worn middle part is approximately the width of the glass layer on the dicing street. The reason behind the deformed blades is probably that the blade wears differently when cutting glass and silicon.

Figure 59 Blade profile inspection of the first cut blades of the optimization DOE.

The problem of first blade shifting was realized when the first wafer was diced in production conditions. This became a new challenge that arose along the step cut process. No blade breakage had occurred during optimization DOE trials so this was an unexpected outcome. The Z1 blade started to tilt during dicing and finally it was broken. It seemed that the blade load during first cut was too high because the blade had started to bend and the alignment had moved before the blade broke down. A reason behind blade bending and shifting might be a too large blade exposure. The first cut blade used in these trials had a larger outer diameter and blade exposure than is usually recommended by the manufacturer. A smaller exposure could make the blade more stable and accurate. Further experimentation is recommended to improve the accuracy of the dicing kerf.

4 Conclusions

Through characterizing the step cut dicing process, the effects of different process variables to process outputs were defined. Significant increase in dicing quality was achieved by optimizing the process parameters. Especially the level of back side chipping was successfully decreased. The optimal process parameter combination for the step cut process that was defined in this research was a metal bond blade, step depth 1/3, feed rate 7 mm/s, and spindle speed 35 000 rpm for Z1 and 27 000 rpm for Z2.

Blade type selection was found to be a critical stage in optimizing the dicing process. Significant differences in back side chipping levels were found with the two different 2nd cut blades that were tested. Back side chipping was reduced by using a metal bond blade. The metal bond blade had larger grit size, lower concentration and softer bond material than the nickel bond blade. Nickel bond blade's cutting ability was not sufficient enough to reduce back side chipping.

Feed rate and step depth both affected front side chipping and back side chipping differently. A lower feed rate was more beneficial for front side quality whereas a higher feed rate was better for back side quality. A deeper step depth improved front side but not back side quality. Reducing back side chipping was the most important quality improvement target so the parameters were chosen primarily according to which one gave the best back side quality. The conclusion for a suitable spindle speed was that a high spindle speed was the best option for good front side quality whereas a low speed gave the best back side quality so the spindle speeds were adjusted separately for Z1 and Z2.

Blade wear and spindle current both increased with a low spindle speed, a high feed rate and thicker cutting substrate. No excessive blade loading was observed in any of the trials according to the spindle current values which stayed reasonable in all of the experimental runs. Spindle current values decreased during dicing which indicates that the blades cutting ability increased when the dicing proceeded.

A new challenge that came up in the experiments for step cut dicing was the poor accuracy of the dicing kerf. A smaller blade exposure would potentially increase the blade's stability so that it would be able to cut the wafer without bending. For further studies a first cut blade

with a smaller outer diameter is suggested to eliminate the shifting of the dicing kerf. The optimized step cut process could be applied into production after resolving this issue.

To further improve the process it would be beneficial to widen out the range of variables included in the process characterization. It is under interest to study the effect of the variables that were left out of this research because it is extremely likely that they would have considerable effects on the output as well. For example the effect of a different mounting tape to back side chipping and die stability is under high interest. If the dicing process characterization would be extended it would be worthwhile to develop more accurate measurement methods for the outputs. Valuable information about blade loading and its effect on dicing quality could be gained from process controls such as blade temperature or blade torque monitoring. More detailed inspections of the correlation between spindle current and chipping levels should be done if spindle current were wished to be utilized as an indicator of process performance. Reducing the wafer back side residual stresses could also be an alternative way to improve back side chipping. Processes such as chemical wet-etch or atmospheric down-stream plasma etching have been suggested to remove stressed layers and scratches which work as stress risers [20].

References

1. Yoshida, K., Murata Combines Precision, Reliability in MEMS Sensor, 2012, Available from: www.murata.com/~/media/webrenewal/about/newsroom/tech/sensor/mems/ta1292.ashx?la=en-us, 11.5.2015.

2. Spearing, S.M., Materials Issues in Microelectromechanical Systems (MEMS), *Acta Materialia*, 2000, **48** (1) 2000, pp. 179-196, ISSN 1359-6454.

3. McCabe, P., Sawing Silicon. *Advanced Packaging*, **14** (3) 2005, pp. 26-27, ISSN 10650555.

4. Lei, W., Kumar, A. and Yalamanchili, R., Die Singulation Technologies for Advanced Packaging: A Critical Review, *Journal of Vacuum Science and Technology B:Nanotechnology and Microelectronics,* **30** (4) 2012, ISSN 21662746.

5. Ganesh, V.P. and Lee, C., Overview and Emerging Challenges in Mechanical Dicing of Silicon Wafers, *Electronics Packaging Technology Conference, 2006. EPTC '06. 8th*, Singapore 2006, pp. 15-21, DOI 10.1109/EPTC.2006.342684.

6. Weisshaus, I., Shi, D. and Efrat, U., Wafer Dicing, Available from: http://electroiq.com/blog/2000/01/wafer-dicing/, 10.6.2015.

7. Kuisma, H., MEMS-teknologia, Available from: http://www.muratamems.fi/fi/murata/murata-electronics-oy/mems-teknologia, 14.5.2015.

8. Anonymous, Murata Electronics Oy Tuotteet, Available from: http://www.muratamems.fi/fi/tuotteet, 13.5.2015.

9. Anonymous, 3D MEMS A State of the Art Technology for the Future, Available from: http://www.murata.com/en-eu/products/sensor/inclinometer/techguide/3dmems, 26.5.2015.

10. Franssila, S., *Introduction to Microfabrication (2nd Edition),* Hoboken, NJ, USA: John Wiley & Sons, 2010, p. 536, ISBN 9780470666722.

11. Sullivan, S. Dicing of MEMS Devices, In *Handbook of silicon based MEMS materials and technologies (1st Edition)*, edited by Lindroos, V., Tilli, M., Lehto, A. and Motooka, T., 2010, pp. 601-606, ISBN 978-0-8155-1594-4.

12. Levinson, G., Principles of Dicing, Available from: http://www.adt-co.com/ADT//userdata/SendFile.asp?DBID=1&LNGID=1&GID=607, 14.3.2015.

13. Anonymous, Product Information - Fully Automatic Dicing Saw, Available from: http://www.disco.co.jp/eg/products/dicer/, 3.6.2015.

14. Shah, H. and Ram, S. Characterization of the Wafer Dicing Process using Taguchi Methodology, *Advanced Semiconductor Manufacturing Conference and Workshop, 1992. ASMC 92 Proceedings*, Cambridge 1992, pp. 200-205, ISBN 0-7803-0740-2.

15. Efrat, U., Optimizing the Wafer Dicing Process. *Electronic Manufacturing Technology Symposium, 1993, Fifteenth IEEE/CHMT International*, Santa Clara 1993, pp. 245-253, ISBN 0780314247.

16. Levinson, G., Process Optimization of Dicing Microelectronic Substrates, Available from: http://www.adt-co.com/ADT//userdata/SendFile.asp?DBID=1&LNGID=1&GID=588, 3.4.2015.

17. Gatzen, H.H., Dicing Challenges in Microelectronics and Micro Electro-Mechanical Systems (MEMS), *Microsystem Technologies*, **7** (4) 2001, pp. 151-154, ISSN 09467076.

18. Weisshaus, I. and Shi, D., Wafer Dicing Step by Step - Step 1: The Back-End Process, Available from: http://electroiq.com/blog/2001/01/step-1-the-back-end-process/, 25.5.2015.

19. Paydenkar, C., Poddar, A., Chandra, H. and Harada, S., Wafer Sawing Process Characterization for Thin Die (75micron) Applications, *Electronics Manufacturing Technology Symposium, 2004. IEEE/CPMT/SEMI 29th International*, 2004, pp.74-77, ISBN 1089-8190.

20. Lyman R.C., Brown, M., Evans, S., Bedore, S., Gutentag, C.E. and Sierra, R.A., Wafer Finishing—Dicing,Picking,Shipping, In *Area Array Interconnection Handbook*, edited by Puttlitz, K.J. and Totta, P.A., Springer US, 2001, pp. 201-227, ISBN 978-1-4615-1389-6.

21. Cheung, A.T., Dicing Advanced Materials for Microelectronics, *Advanced Packaging Materials: Processes, Properties and Interfaces, 2005. Proceedings. International Symposium*, Irvine 2005, pp. 149-152, ISBN 0780390857.

22. Anonymous, Electroformed bond blades, Available from: http://www.disco.co.jp/eg/products/catalog/pdf/zp07.pdf, 9.5.2015.

23. Abdullah, S., Yusof, S.M., Jalar, A., Abdullah, M.F., Aziz, Z.A. and Daud, R., Step Cut for Dicing Laminated Wafer in a QFN Package, *Solid State Science and Technology*, **16** (2) 2008, pp. 198-206, ISSN 0128-7389.

24. Shi, K.W., Yow, K.Y. and Khoo, R., Developments of Blade Dressing Technique using SiC Board for C90 Low-K Wafer Sawing, *Electronics Packaging Technology Conference (EPTC), 2011 IEEE 13th*, Singapore 2011, pp. 122-128, ISBN 9781457719837.

25. Levinson, G., Introduction to Dressing, Available from: http://www.adt-co.com/ADT/Templates/showpage.asp?DBID=1&LNGID=1&TMID=84&FID=932, 15.4.2015.

26. Shi, K.W., Yow, K.Y. and Khoo, R., Investigations of the Effects of Blade Type, Dicing Tape, Blade Preparation and Process Parameters on 55nm Node Low-K Wafer, *Electronic Manufacturing Technology Symposium (IEMT), 2010 34th IEEE/CPMT International*, Melaka 2010, pp. 1-6, ISBN 10898190.

27. Luo, S.Y. and Wang, Z.W., Studies of Chipping Mechanisms for Dicing Silicon Wafers, *International Journal of Advanced Manufacturing Technology*, **35** (11-12) 2008, pp. 1206-1218, ISSN 02683768.

28. Arif, M., Rahman, M. and San, W.Y., A State-of-the-Art Review of Ductile Cutting of Silicon Wafers for Semiconductor and Microelectronics Industries, *The International Journal of Advanced Manufacturing Technology*, **63** (5-8) 2012, pp. 481-504, ISSN 1433-3015.

29. Jasinevicius, R.G., Porto, A., Pizani, P., Duduch, J. and Santos F., Characterization of Structural Alteration in Diamond Turned Silicon Crystal by Means of Micro Raman Spectroscopy and Transmission Electron Microscopy, *Materials Research*, **8** (3) 2005, pp. 261-268, ISSN 1980-5373.

30. Lin, J. and Cheng, M., Investigation of Chipping and Wear of Silicon Wafer Dicing, *Journal of Manufacturing Processes*, **16** (3) 2014, pp. 373-378, ISSN 1526-6125.

31. MFI internal material.

32. Hooi, T.E., Nyen, C.F. and Tsun, L.W., What's Next After Process Characterization, *Electronic Manufacturing Technology Symposium, 2007. IEMT '07. 32nd IEEE/CPMT International*, San Jose, CA 2007, pp. 8-13, ISBN 10898190.

33. Allen, J.J., *Micro Electro Mechanical System Design*, Boca Raton, FL: Taylor & Francis, 2005, p. 465, ISBN 0-8247-5824-2.

34. Huang, S. and Pan, Y., Automated Visual Inspection in the Semiconductor Industry: A Survey, *Computers in Industry*, **66** 2015, pp. 1-10, ISSN 0166-3615.

35. Antony, J., *Design of Experiments for Engineers and Scientists*, Jordan Hill, GBR: Butterworth-Heinemann, 2003, p. 165, ISBN 9780080469959.

36. Eriksson, L., Johansson, N., Kettaneh-Wold, C., Wikström, C. and Wold, S., *Design of Experiments: Principles and Applications (3rd Edition),* Umeå, SE: MKS Umetrics AB, 2008, p. 459, ISSN 9197373044.